Research Square

Preprints are preliminary reports that have not undergone peer review.
They should not be considered conclusive, used to inform clinical practice,
or referenced by the media as validated information.

Targeting MRE11 Overcomes Platinum Resistance and Enhances Radiosensitivity in Non-Small Cell Lung Cancer Cells

Bahadır Yasin Erol
University Hospital Essen
Ali Sak
ali.sak@uk-essen.de

University Hospital Essen
Maja Guberina
University Hospital Essen
Jürgen Thomale
University Hospital Essen
Georg Iliakis
University Hospital Bonn
Martin Stuschke
University Hospital Essen

Research Article

Keywords: cisplatin, radiation, NSCLC, DNA damage response, radiosensitization, MRE11, mirin

Posted Date: November 6th, 2026

DOI: https://doi.org/10.21203/rs.3.rs-11137986/v1

License: This work is licensed under a Creative Commons Attribution 4.0 International License.
Read Full License

Additional Declarations: No competing interests reported.

Targeting MRE11 Overcomes Platinum Resistance and Enhances Radiosensitivity in Non-Small Cell Lung Cancer Cells

Running title: Targeting MRE11 to Overcome NSCLC Resistance

Erol BY[1#], Sak Ali[1*#], Guberina M[1], Thomale J[2], Iliakis G[3], Stuschke M[1].

[1]Department of Radiation Therapy, University Hospital Essen, Essen, Germany

[2]Institute for Cell Biology, University Hospital Essen, Essen, Germany

[3]Department of Radiation Therapy, University Hospital Bonn, Bonn, Germany

***Ali Sak, PhD**
Tel.: +49201-7232818; Fax: +49/201-7235960
e-mail: ali.sak@uk-essen.de

Erol Bahadır Yasin, PhD
e-mail: yasinbahadirerol@gmail.com

Jürgen Thomale, PhD, PD
e-mail: juergen.thomale@uk-essen.de

Georg Iliakis, PhD, Prof.
e-mail: georg.iliakis@uk-essen.de

Maja Guberina, MD, PD
e-mail: maja.guberina@uk-essen.de

Martin Stuschke, MD, Prof.
e-mail: martin.stuschke@uk-essen.de

*Corresponding author

Department for Radiotherapy, University Hospital Essen

Hufelandstr 55, 45122 Essen, Germany

shared 1st authorship

Abstract

Purpose: Concomitant cisplatin (CP)-based chemo-radiotherapy is a standard-of-care regimen for non-small cell lung cancer (NSCLC), but intrinsic and acquired resistance to CP and ionizing radiation (IR) severely limits clinical efficacy. The MRN complex is essential for DNA double-strand break (DSB) repair and coordinates the cellular response to both IR-induced lesions and CP-mediated crosslinks. This study investigated the interaction between CP-induced adduct formation and IR-driven DSBs, evaluating whether inhibiting the MRE11 subunit of the MRN complex can selectively reverse resistance and enhance chemo-radiosensitivity in platinum-resistant NSCLC.

Methods: A panel of nine NSCLC cell lines and two non-transformed human dermal fibroblast models were examined. Cellular responses to CP, IR, or their combination were evaluated via clonogenic survival and cell cycle analysis. Pt-GpG crosslink kinetics were quantified, and the DNA damage response (DDR) was monitored by tracking γH2AX, 53BP1, and RAD51 foci formation. Pharmacological MRE11 inhibition was achieved using the small-molecule inhibitor mirin.

Results: Based on 72-hour half-maximal inhibitory concentrations, IC50, NSCLC lines were stratified into CP-sensitive (IC50≤ 2μM) and CP-resistant (IC50> 2μM) cohorts. CP significantly enhanced the radiosensitivity of the most CP sensitive cell lines, without an effect on radiosensitivity cell lines resistant for cisplatin. Initial Pt-GpG adduct burden did not correlate with baseline CP sensitivity. While CP triggered S- and G2/M-phase arrest across all lines, mirin selectively enhanced the radiosensitivity of CP-resistant NSCLC cells (A549, H1299, H838, H520, and H23; with the exception of H1975). Mechanistically, mirin significantly elevated Pt-GpG adduct retention and disrupted downstream DDR signaling (53BP1 and RAD51 foci formation) in these resistant tumor cells. In stark contrast, mirin significantly reduced adduct accumulation and slightly increased post-irradiation survival in normal fibroblasts, leaving their primary DDR signaling intact.

Conclusions: MRE11 inhibition via mirin selectively disrupts DDR signaling and promotes cisplatin-adduct retention in platinum-resistant NSCLC cells while sparing non-transformed tissues. These findings establish MRE11 as a promising therapeutic target to overcome chemo-radioresistance in refractory lung carcinomas while protecting normal cells.

Key words: cisplatin, radiation, NSCLC, DNA damage response, radiosensitization, MRE11, mirin

Introduction

Lung cancer remains the leading cause of cancer-related mortality worldwide, with non-small cell lung carcinoma (NSCLC) accounting for approximately 85% of all cases [1]. Despite advances in targeted therapies and immunotherapy, CP-based chemotherapy, in combination with ionizing radiation, remains the standard of care for advanced NSCLC, particularly in patient's ineligible for surgical resection [2]. However, the effectiveness of CP-based chemo-radiotherapy is often hindered by intrinsic or acquired resistance [1-3], leading to poor treatment responses and high recurrence rates [4].

The therapeutic activity of cisplatin is facilitated by an active species, created by aqueous hydrolysis as the drug enters the cell. This active species interacts with DNA, RNA, protein, membrane phospholipids, microfilaments and thiol-containing molecules. However, the cytotoxic effect appears to be mainly facilitated through the formation of DNA inter- and intra-strand crosslinks [5], where intra-strand guanine-guanine (GpG) crosslinks represents about 65% of all adducts [6]. Adduct formation leads to replication fork stalling, DNA damage and apoptosis [5,7]. However, cells can develop resistance through several mechanisms, including reduced intracellular CP accumulation, increased drug efflux [8], improved repair of CP adducts and enhanced tolerance of the subsequent DNA damage [9-11]. In addition, alterations in apoptotic signaling via mutations in p53 and BCL-2 family proteins [12] also enable cells to evade the cytotoxicity of cisplatin.

In comparison, IR creates clusters of damage consisting of various DNA lesions, such as double- and single-strand breaks, as well as base lesions [13]. Therefore, combined treatment with cisplatin and IR could potentially increase the complexity of induced DNA damage, which could have an important impact on the choice of repair pathways. Consequently, there is growing interest in understanding how combined treatment schedules affect DNA damage repair and how therapeutics can improve the initial tumour response and overcome acquired drug or radiation resistance.

The cellular response to DNA damage induced by IR or cisplatin consists of sensing the damage by sensor proteins such as the MRE11-RAD50-NBS1 (MRN) complex and DNA-

PK. These sensor proteins then initiate a signal transduction cascade, involving the activation of key checkpoint regulators and DNA-damage response transducing kinases, such as ataxia-telangiectasia-mutated (ATM) and ataxia-telangiectasia and Rad3-related (ATR) [14,15].

The MRN complex is a key regulator of the DNA damage response, particularly in double-strand break repair via homologous recombination repair (HRR) and non-homologous end joining (NHEJ) [16]. MRE11 is a core component of the MRN complex, acting as a critical sensor and processor for DSBs. It possesses two distinct catalytic activities that are both essential for DNA repair: the 3'-5' exonuclease activity and the endonuclease activity. The exonuclease activity trims the ends of DNA strands to clean up dirty DNA ends, while the endonuclease activity is essential for DNA end resection, which creates overhangs and thus required for homologous recombination.

Mirin is a potent small-molecule inhibitor that targets the MRE11 active site. By inhibiting both the exo- and endonuclease functions, it prevents the initial processing of DSBs and the MRN dependent activation of the ATM kinase [17, 18], which effectively halts the downstream DNA damage response signaling. Studies suggest that many CP-resistant NSCLCs rely on MRE11-mediated HRR for survival, making it a potential therapeutic target [17]. The MRN complex also acts as a "bridging unit" in DNA repair by using the RAD50 coiled-coil arms to physically link distant DNA ends, which is critical for repairing double-strand breaks (DSBs) caused by radiation and inter-strand crosslinks from cisplatin. This bridging is a key function that allows for efficient signaling and repair by bringing the broken ends together for proper ligation and DNA damage response activation. This tethering is a crucial step in activating cell cycle checkpoints, such as those mediated by ATM kinase, ensuring that cells don't proceed with division until the damage is repaired. The combination of cisplatin and radiation can be more damaging, creating complex lesions that heavily rely on the MRN complex for their repair. Because of its essential role in combined treatment schedules with CP and IR, targeting the MRN complex is being explored as a way to increase the effectiveness of radio-chemotherapy by making cancer cells more sensitive to treatment.

Thus, we hypothesize that inhibiting the MRE11 could impair the DDR efficiency of CP-resistant NSCLC cells, thereby increasing their sensitivity to CP and IR. To test this hypothesis, we first characterized NSCLC cell lines based on their sensitivity to CP. We then explored CP-induced DNA damage and repair mechanisms, and assessed the effects of MRE11 inhibition with mirin, a potent small-molecule inhibitor that inhibits both the exo- and endonuclease functions, on radiosensitisation in tumour cells and non-transformed fibroblasts, in order to evaluate tumour selectivity.

Methods

Cell lines, cell culture and Irradiation

The human non-small cell lung carcinoma NSCLC cell lines H460, H661, A549, H1299, H1975, H838, H522, H520, H23 were used. Some of the reported genetics variations in these cell lines include TP53 (H1299, H661, H1975, H838, H522, H520, H23), KRAS (H460, A549, H23), ATM (H520 heterozygous, H23 homozygous) and ATR (H661) mutations. Data obtained from The Broad Institute of MIT & Harvard (portals.broadinstitute.org/ccle). The cell lines were obtained from American Type Culture Collection (ATCC, Rockville, MD, USA). The A549 cell line was maintained in MEM (Invitrogen) supplemented with 15% FBS plus 1% non-essential amino acids and antibiotics. The rest of the cell lines were maintained in RPMI1640 (Invitrogen, Paisley, UK) supplemented with 10% FBS plus antibiotics. Adult dermal fibroblasts (HDFA, PCS-201-012) and neonatal dermal fibroblasts (HDFN, PCS-201-010) were cultivated in fibroblast basal medium (FBM, PCS-201-030, ATCC), and supplemented with low serum fibroblast growth kit (ATCC, PCS-201-041). All cell lines were propagated in medium supplemented with 5 µg/ml plasmocin (InvivoGen, Toulouse, France) as a mycoplasma prophylaxis and were cultivated in an atmosphere consisting of 5% CO2 and 95% air at 37 °C. Cell lines were usually re-thawed after 3 months in culture. Cells were irradiated using an X-ray machine RS320 (X-Strahl Ltd, Surrey, UK) at 300 kV, 10 mA, dose rate 1.1 Gy/min.

Proliferation assay

All NSCLC cells were harvested and plated at a density of 3×10^5 cells per well in 6-well (9.6 cm2/well) cell culture plates (except for H661 $1,5 \times 10^5$). After 24 h the cells were treated with the desired reagents for durations as indicated. The cells were trypsinized and counted at 24 h, 48 h and 72 h after treatments using the automated cell counting system Luna (logos biosystems, Korea). The IC50 represents the concentration of CP required to reduce the total number of viable cells by 50% compared to the untreated controls and was estimated by a three-parameter logistic model fit using the SAS NLMIXED procedure (SaS. 1999; Lyles et al. 2008).

Clonogenic survival assay

For the measurement of clonogenic survival, all NSCLC cells were plated at a density of 3 × 105 cells per well in 6-well (9.6 cm2/well) cell culture plates (except for H661 1,5 × 105) for 24 h. The next day after the treatments that are explained in the next paragraph in detail, cells were plated in triplicates at a density of 100-10000 cells per well depending on the irradiation dose and treatment conditions and colonies were counted by hand after 10-18 days of incubation. To examine the effect of Cisplatin or Mirin on clonogenic survival, cells were treated with Cisplatin (0–5 μM) or Mirin (20 μM) for indicated times. To investigate the radiosensitizing effects of Cisplatin, cells were irradiated with single doses of 0–6 Gy after 4 h of Cisplatin (0–5 μM) treatment. To test whether Mirin has an influence on the radiosensitizing effect of Cisplatin, cells were treated with Mirin for 24 h followed by Cisplatin (0-5 μM) for another 4 h. Cells were plated in 6-well plates at a density of 100–1000 cells per well and irradiated with single doses of 0–6 Gy. After 48 h Mirin treatment, the media was changed and colonies were allowed to form at 37 °C in 5% CO2 for 10–18 days. Cells were fixed and stained (with 96% ethanol, 15% (w/v) Giemsa) and destained with distilled water. Colonies were counted that had more than 50 cells. The surviving fractions after the respective radiation dose are presented as a fraction of the growth of untreated colonies.

Transfection with siRNA

24h before transfection, cells were plated into 8-well (0.69 cm2) chamber slides ($1{,}5x10^5$ cells/chamber) for immunofluorescence analysis or 6 well culture plates ($0.4x10^6$ cells/well) with the respective growth medium for western blotting assay. Optimal cell density was optimized to reach 60-80% at the time of transfection. For each transfection sample, Lipofectamine® RNAiMAX reagent was diluted in Opti-MEM® (Gibco) without serum, antibiotics and antimycotics and mixed gently. The cells were incubated for 48 h at 37°C in 5% CO2.

Immunoblotting

Cells were harvested and lysed in RIPA buffer (Thermo, Rockford, USA) supplemented with a 1x protease inhibitor cocktail (Roche, Mannheim, Germany) for 15 minutes at 4 °C. Equal amount of protein lysates were mixed with 4xLDS sample buffer (Invitrogen, Carlsbad, USA) and heated to 95 °C for 5 min prior to gel loading. After separation by NuPAGE 4–12% bis-tris or 7% tris-acetate gels (Invitrogen), proteins were transferred to PVDF blotting membranes (Invitrogen, CA, USA). Membranes were blocked in 5% defatted powdered milk/Tris–buffered saline 0.5% Tween 20 at room temperature for 1 h and incubated with the primary antibody overnight at 4 °C. After washing, the membranes were incubated with the secondary antibody conjugated with horseradish peroxidase and visualization was performed using SuperSignal West FemtoStable Peroxide Buffer and Luminol/Enhancer Solution (Thermo). ChemiDOC MP Imaging System (Biorad) was used for signal detection. The following antibodies were used: mouse mAb anti-ERCC1 1:1000 (Sc17809, Santa Cruz Biotechnology), 1:1000 (2531, Cell Signalling), anti-rabbit IgG HRP-linked 1: 5000 (7074P2, Cell Signalling), rabbit pAb to GAPDH 1: 2000 (ab9485, abcam) or mouse mAb to GAPDH 1: 2000 (ab8245, abcam).

Immunofluorescence microscopy

Cells were grown onto 4- or 8-wells chamber slides. After treatment, cells were fixed with 4.5% formaldehyde for 20 min, permeabilized for 15 min in permeabilising buffer (100 mM Tris-HCl, pH 7.4; 50 mM EDTA, 0.5% Triton X-100) and thereafter blocked for 1 h at room temperature in the blocking solution (3% BSA, 0.1% Tween 20, 4xSSC). Cells were then incubated with the primary antibodies, i.e. rabbit anti-Rad51 1:500 (PC130-100, Calbiochem), rabbit anti-53BP1 1:500 (ab21083, abcam) and mouse anti γ-H2AX 1:500 (ab22551, abcam) overnight at 4 °C. The secondary antibodies goat anti-rabbit Cy3-conjugated antibody 1:500 (800-367-52, Jackson Immuno Research) and Alexa Fluor 488 goat anti-mouse 1:500 (A11017, life technologies) were applied together with 4′-,6-diamidino-2-phenylindole DAPI nuclear counterstain 1 µg/ml for 1 h at room temperature. Images were obtained using a fluorescence microscope Imager Z1 (Zeiss; Jena, Germany).

Measurement of Cisplatin-DNA adducts

Cisplatin-DNA adducts in NSCLC cells were measured as previously described (Barr et al. 2013), with minor modifications. Briefly, cells were directly cultured and grown onto the Superfrost Gold Slides (ThermoFisher). Cells were treated with different concentrations of Cisplatin for 4 h, washed with PBS and cultured for further 20 h in drug free medium. After treatment, cells were fixed for 30 min in ice-cold methanol and subjected to proteolytic digestion with 60 µg/mL pepsin and 40 µg/mL proteinase K. Cells were blocked with non-specific binding sites with 5% (w/v) non-fat powdered milk in PBS at 37 °C and incubated at 4 °C overnight with a rat primary antibody (1:500) that specifically recognizes Cisplatin-GpG DNA adducts (RC-18). The secondary antibodies (anti-rat Cy3®-labelled antibody 1:500; Dianova, Hamburg) were applied together with 4′-,6-diamidino-2-phenylindole DAPI nuclear counterstain 1 µg/ml (w/v) for 1 h at room temperature. Images were acquired on an Axioplan fluorescence microscope (Carl Zeiss GmbH, Göttingen, Germany). For the quantification of Cisplatin-GpG (CP-GpG) DNA adducts, fluorescence signals were measured by quantitative digital image analysis using the ACAS 6.0 CytometryAnalysis System (ACAS II, Ahrens Electronics, Bargterheide, Germany). Levels of adducts in each sample were calculated as arbitrary fluorescence units (AFU's), upon normalization of the integrated antibody-derived fluorescence from more than 100 individual nuclei/ sample to the corresponding DNA content. Data are presented as the mean AFU ± 95% confidence interval (CI) from three to four independent experiments.

Flow cytometry and Cell Cycle Analysis

For cell cycle analysis, samples were washed once with PBS and then fixed with 70% EtOH overnight at 4°C. For the FACS analysis the fixed samples were washed once with PBS and then stained with DAPI (1µg/ml) in PBS overnight. The following day the samples were filtered and the cell cycle distribution was analysed with the FloMax and MultiCycle ver.3.0 software.

Statistical analysis

All data were expressed as the mean ± standard error of the mean (S.E.M.). The statistical analysis of colony assays was performed by Nonlinear Regression (curve fit), and the means of two data sets were compared by a student's t-test using the GraphPrism 6 software (GraphPad, La Jolla, CA, USA). For each drug exposure combination, the ratio of counted colonies versus seeded cells at each radiation dose group was normalized by the plating efficiency of unirradiated control cells at the same drug exposure condition. The dependent observations were the logarithms of these normalized ratios from each experiment with at least three cell culture plates. The significance of an independent variable was assessed by Nonlinear Regression. Statistical significance was set at a level of alpha = 0.05. In order to obtain statistically relevant results from measurement of Cisplatin-GpG DNA adduct level experiments, at least 100 cells were analyzed from each sample for the calculation of the means and the variance. The results were presented graphically using the GraphPad Prism 6 program. The error bars shown represent the 95% confidence interval, the probability range around the calculated mean, in which this is 95% with an infinite sample size. Nonlinear Regression (Curve Fit) was used for statistical analysis. The significance of the results of a statistical analysis is given as a p-value (probability). The significance level was set at 5% ($p = 0.05$), the smaller the p-value, the more significant the result (*$p<0.05$, **$p<0.01$, ***$p<0.001$, ****$p<0.0001$).

Results

Effect of cisplatin on proliferation of NSCLC cell lines

To classify the NSCLC cell lines based on their cisplatin (CP) sensitivity, proliferation assays were performed using clinically relevant concentrations (1, 2, and 5 μM). CP treatment reduced cell proliferation in a time- and concentration-dependent manner across all cell lines (figure 1, supplemental figure S1). IC50 values calculated 72 hours post-washout ranged from 1.2 μM to 4.4 μM (table 1). Based on these values, cell lines were categorized into two groups: CP-sensitive (S; IC50 ≤ 2 μM: H460, H661, H522) and CP-resistant (R; IC50 > 2 μM: A549, H1299, H1975, H838, H23, and H520).

Effect of cisplatin on cell cycle distribution of NSCLCs

To evaluate the impact of CP on cell cycle progression, flow cytometry was performed. Cells were treated with 1, 2, or 5 μM CP for four hours, fixed at 0-, 24-, and 48-hours post-washout, and analyzed. Across all cell lines, CP induced a concentration-dependent accumulation of cells in the S and G2/M phases at 24- and 48-hours post-washout (supplemental figure S2). Specifically, G2/M-phase arrest was most pronounced in H460 cells, whereas H661 cells exhibited the highest S-phase accumulation. However, no generalized correlation was observed between cisplatin sensitivity (S/R status) and the specific pattern of cell cycle alterations.

Effect of cisplatin on radiosensitivity of NSCLC cell lines

The cells were exposed to 2 μM CP for a period of 4 hours, after which the cells were plated for colony formation. Following a 4 - 6 h recovery period from the effects of trypsin, the colonies were irradiated with 0, 2, 4 and 6 Gy, and, depending on the cell line, left to incubate for approximately 10 to 18 days. Cisplatin significantly enhanced the radiosensitivity of the most CP sensitive cell lines H460, H661 and H522 (figure 2, supplemental figure S3). However, no differences in radiosensitivity were observed between the control and cisplatin-treated groups in the other cell lines (A549, H1299, H1975, H838, H23 and H520).

Effect of cisplatin on induction and repair of IR induced DNA-DSBs

In order to analyse the effect of cisplatin on radiation-induced DSB repair signalling, γH2AX was utilised as a measure of global repair signalling and RAD51 as a marker for HRR activity. In order to achieve this objective, the cells were subjected to concentrations of cisplatin ranging from 1 µM to 120 µM for a duration of 4 hours. Thereafter, they were irradiated with 0, 2, or 4 Gy. Subsequently, the cells were fixed at 1 hour, 4 hours and 24 hours. The data demonstrate that concentrations of cisplatin greater than 15 µM significantly decrease the formation of radiation induced γH2AX (figure 3, supplemental figure S4), while concentrations greater than 30 µM also decreased Rad51 foci (figure 4, supplemental figure S5).

Formation of cisplatin adducts in NSCLCs

Measuring the formation of cisplatin adducts can further help to characterize the sensitivity NSCLC lines to cisplatin. To this end, an antibody that recognizes cisplatin-guanine-guanine intra-strand adducts (Pt-GpG) was used (figure 5). The staining intensity of Pt-GpG intra-strand adducts at 24 h after washout of 4 h CP treatment increased with increasing CP concentrations (supplemental table S1). There was no correlation between Pt-GpG crosslink formation at 30 µM CP and IC50 in the growth assay (r = -0,2580) as well as clonogenic survival after treatment with 2 µM CP (r = -0,3712).

Effect of cisplatin on Mre11 driven radiation sensitivity

In order to study the effect of cisplatin on Mre11-driven survival, cells were treated with mirin, a specific inhibitor of Mre11. Initially, cell proliferation assays were performed to determine the working concentration for subsequent experiments. In order to achieve this objective, cells were exposed to varying concentrations of mirin (0–100 µM) for a period of two days. Thereafter, the number of viable cells was counted. Following a thorough evaluation of the results, 20 µM mirin treatment was selected for subsequent experiments, as this concentration represented the upper limit that could be used in all cell lines without significantly reducing proliferation (supplemental figure S6). In order to analyze the effect of mirin on radiation sensitivity, the cells were treated with 20 µM mirin for a period of 20 hours, followed by a 4-hour treatment with 2 µM of cisplatin. Subsequently, the cells were

plated in media containing 20 μM mirin only and then left to reattach for a period of 4-5 hours prior irradiation. The following day, the medium containing the mirin was substituted with a standard medium without mirin and the cells were left to incubate for a period of 10 – 18 days. Mirin significantly increased the radiation sensitivity of cell lines that were more resistant to cisplatin (A549, H1299, H520 and H23), with the exception of H1975 and H838 (figure 6, supplemental figure S7). Conversely, no significant differences were observed between the control and mirin-treated groups of the most cisplatin-sensitive cell lines (H460, H661 and H522). However, combined treatment with cisplatin, mirin and IR significantly decreased the surviving fraction in all cell lines, except H1975. To further analyze these outcomes following the downregulation of Mre11 with siRNA instead of an inhibitor, experiments were performed on cisplatin-sensitive (H460) and more resistant (A549) cell lines. Transfection with siRNA targeting MRE11 significantly reduced the clonogenic survival of both cell lines. Additionally, combined treatment with siRNA and cisplatin significantly reduced the clonogenic survival of both cell lines (supplemental figure S8).

Effect of mirin on CP adduct formation and DSB repair.

The results of the clonogenic survival assay show that cisplatin-sensitive and -resistant cells responded differently to mirin treatment. To examine whether CP-DNA adduct formation was also affected by mirin, the staining intensity of the Pt-GpG DNA adduct was scored. For this endpoint, the cells were treated with 20 μM mirin, followed by CP for four hours. After the cisplatin treatment, the cells were washed and supplied with mirin-containing media. Slides were fixed at 4, 8, 12 and 24 hours after the start of cisplatin treatment, and the kinetics of CP-DNA adducts were obtained (figure 7, supplemental figure S9 and table S1). Mirin significantly increased adduct formation in cell lines that are more resistant to cisplatin (A549, H1299, H838, H520 and H23), again with the exception of H1975. However, no significant increase was observed in cell lines that were more sensitive to cisplatin (H460, H661 and H522).

With respect to DSB repair signalling, the formation of 53BP1 repair foci for overall repair (mainly NHEJ) and RAD51 repair foci for HRR were evaluated. The data show that

combined treatment significantly reduced the initial formation of 53BP1 only in cell lines that are more resistant to cisplatin (A549, H1299, H838, H520 and H23), with the exception of H1975 (figure 8, supplemental figure S10). By contrast, no significant changes were observed in cell lines that were more sensitive to CP treatment (H460, H661 and H522).

Analysis of RAD51 foci scoring in G2 cells, as determined by Cyclin B1 co-staining, shows that mirin alone significantly decreased initial RAD51 foci formation at 4 hours after IR in the A549, H23, H520 and H522 cell lines (figure 9, supplemental figure S11). Additionally, combined treatment significantly reduced initial RAD51 foci formation in all cell lines, except H661.

Effect of cisplatin, mirin and combined treatment on normal fibroblast cells

To test the effects of combined treatment schedules on normal cells, two human dermal fibroblast cell cultures were used: adult (PCS-201-012) and neonatal (PCS-201-010) fibroblasts. Initially, the effects of cisplatin, mirin, IR and combined treatment on clonogenic survival were evaluated. Cells in the plateau phase (cultured for 72 hours) and exponentially growing cells (cultured for 24 hours) were treated with 20 μM mirin for 20 hours, followed by a 4-hour treatment with 2 μM cisplatin. After wash-out, the cells were then re-plated in media containing 20 μM mirin and left to reattach for 4–5 hours prior to irradiation with 2 Gy. The next day, the mirin-containing medium was replaced with normal medium and the cells were incubated for colony formation. Combined treatment with mirin and cisplatin shows a trend towards an increased surviving fraction in all treated groups, even though these findings were not significant (figure 10).

To determine whether mirin also affects the formation of CP-DNA adducts in fibroblasts, cells containing Pt-GpG adducts were plated onto slides, treated with 20 μM mirin for 20 hours, and then treated with CP (30 μM or 60 μM) for a further 4 hours. After the cisplatin treatment, the cells were washed and supplied with mirin-containing media. Slides were fixed at 4, 8, 12 and 24 hours from the start of the cisplatin treatment, thereby obtaining the kinetics of CP-DNA adducts. The data show different kinetics of adduct formation in

plateau and exponentially growing cells (figure 11). Cells in the plateau phase first accumulate adducts within 12 hours, followed by a slow reduction thereafter. In comparison, exponentially growing cells show a fast accumulation of CP adducts within 4 hours, followed by a fast decline. Interestingly, treatment with mirin significantly decreased CP adduct formation in both plateau and exponentially growing neonatal (HDFN, PCS201-10) and adult (HDFA, PCS201-12) fibroblast cells.

In addition, the effect of cisplatin, mirin and combined treatment on DNA double-strand break (DSB) repair signalling was determined in fibroblast cells. γH2AX and 53BP1 foci were scored to evaluate the effect on overall repair signalling (mainly NHEJ), and RAD51 foci were scored to evaluate HRR repair. Overall, no significant changes were observed in the four groups of cells after the different treatment schedules (control, CP, mirin and CP + mirin), in terms of the initial or residual γH2AX, 53BP1 and Rad51 foci (supplemental figures S12, S13, S14).

Discussion

Study Objectives and Cisplatin Sensitivity Profiling

This study evaluates the impact of cisplatin (CP) and combined chemo-radiotherapy on DNA damage interactions, repair pathways, and radiosensitivity in non-small cell lung cancer (NSCLC) cell lines. The ultimate goal was to identify strategies that enhance the chemo-radiosensitivity of lung carcinomas. Initially, the sensitivity of nine NSCLC cell lines to CP was characterized by examining the impact of clinically relevant concentrations (1–5 µM) on cell proliferation, mirroring the plasma concentrations (3–6 µM) observed in patients [19,20]. The concentrations of CP resulting in 50% inhibition of cell proliferation within 72 h after treatment (IC50) exhibited a range from 1.2 µM to 4.4 µM across the panel of nine non-small cell lung cancer (NSCLC) cell lines. The reduced proliferation of cells in response to CP treatment is predominantly attributable to the induction of cell cycle arrest, specifically in the S and G2/M phases. Cisplatin was found to increase the S- and G2/M-phases in a concentration-dependent manner within 24 hours of CP washout in all cell lines. This, in combination with IR, has the capacity to influence the cells' response to ionizing radiation [21]. It has been reported by several groups that cell cycle arrest occurs in response to CP treatment in a range of cell lines used in the present study, including those that are resistant (A549, H1299, H838, H23 and H520) and those that are sensitive (H522 and H460) to CP treatment [22-25].

DNA Adduct Formation and Correlation with Sensitivity

At the molecular level, cisplatin has been observed to form covalent bonds with DNA, predominantly intra-strand guanine-guanine (GpG) DNA crosslink adducts, with a reported frequency of approximately 65% [26]. These adducts have been demonstrated to impede DNA replication, consequently inducing cell cycle arrest and, in the absence of adequate repair, culminating in cell death [5, 7]. In the present study, a dose-dependent increase in CP-DNA adducts following cisplatin treatment was confirmed. However, concentrations that were comparable to the average clinical dosage of 1–2 mg/L or 3 to 6 µM [19] were found to be indistinguishable from control groups in the present experimental setting. Consequently, the analysis of CP-adduct formation was conducted using higher CP concentrations of 15, 30 and 60 µM, in order to identify inherent

differences between the cell lines. It was observed that the cisplatin-resistant cell lines A549, H1299 and H1975 exhibited a trend to reduced level of CP adduct formation in comparison to the more CP sensitive cell lines. However, no significant correlation between Pt-GpG crosslink formation at 30 µM CP and IC50 in the growth assay (r = -0,2580) as well as clonogenic survival after treatment with 2µM CP (r = -0,3712) was found. An absence of a correlation between CP adduct levels and sensitivity to CP has also been documented in previous studies [23, 27, 28].

Cisplatin-Mediated Radiosensitization is Cell-Line Dependent

Because combining radiotherapy and cisplatin (CP) is a standard clinical regimen for non-small cell lung cancer (NSCLC), this study investigated whether this combination systematically enhances radiosensitivity across various NSCLC cell lines. Our data demonstrate that cisplatin acts as a radiosensitizer exclusively in inherently CP-sensitive cell lines (H460, H661, and H522), whereas no sensitization occurs in more CP-resistant cell lines (A549, H1299, H1975, H838, H23, and H520). This highlights that cisplatin-mediated radiosensitization is not a universal phenomenon but rather cell-line specific, corroborating earlier findings [29, 30]. Specifically, Toulany et al. [30] hypothesized that the lack of radiosensitization in the resistant A549 line stems from CP-induced activation of ataxia-telangiectasia mutated (ATM) signaling and subsequent cytoprotective autophagy. While ATM-driven DNA damage responses also mediate synergy between cisplatin and gemcitabine in bladder cancer [31], our findings challenge the ubiquity of this mechanism. Notably, the ATM-mutated lines H23 (homozygous) and H520 (heterozygous) utilized in this study similarly failed to exhibit CP-mediated radiosensitization, suggesting that functional ATM signaling is not the defining factor in this process. Instead, cell cycle dynamics may dictate this synergy. Qiu et al. [21] recently demonstrated that effective radiosensitization requires cisplatin exposure during the S-phase followed by active cell cycle progression. Consequently, the replication index during drug exposure and the subsequent kinetics of cell cycle progression are most likely the primary determinants of cisplatin-induced radiosensitization.

Cisplatin Interferes with DNA Double-Strand Break Repair Signaling

The most deleterious lesion induced by ionizing radiation (IR) is the DNA double-strand break (DSB), which is primarily repaired via non-homologous end-joining (NHEJ) and homologous recombination repair (HRR). This study investigated whether cisplatin (CP) adducts physically or signaling-wise interfere with DSB repair pathways during combined treatments. Our data demonstrate that CP significantly reduces radiation-induced γH2AX and RAD51 foci formation at concentrations exceeding 15 μM and 30 μM, respectively. These observations align with findings by Sak et al. [32], who reported a similar reduction in initial γH2AX foci formation in lymphocytes post-cisplatin treatment, without affecting the physical rejoining of DNA strands as measured by constant-field gel electrophoresis. Consequently, this reduction in foci formation likely reflects impaired chromatin relaxation and aberrant checkpoint activation induced by CP adducts rather than a decrease in actual DNA breaks [33].

Furthermore, most cell lines in this study showed no substantial alterations in residual foci. A notable exception occurred in the ATM-mutant lines H520 and H23, which exhibited significantly augmented residual γH2AX foci 24 hours post-IR ($p < 0.01$), indicating a severely diminished DNA damage repair capacity. This prolonged retention of damage markers can be attributed to two cooperating factors: first, these specific cell lines possess a significantly slower proliferation rate and require a longer timeframe to complete the cell cycle compared to other fast-growing NSCLC models [25]; second, they lack functional ATM protein [34], a critical upstream kinase required for efficient DSB repair signaling and checkpoint coordination [35].

Targeting MRE11 with Mirin Sensitizes Cisplatin-Resistant NSCLC Cells

As a genotoxic agent, cisplatin (CP) interferes with multiple DNA repair pathways, including the MRN complex. The MRE11 nuclease, a core component of this complex, is pivotal for DNA damage signaling, lesion processing, and stalled replication fork resolution [36]. Downregulation of MRE11 elevates sensitivity to DNA-damaging agents and reduces mismatch repair activity [37]. Consequently, targeting MRE11 has emerged as an attractive strategy for inducing synthetic lethality, as demonstrated by its capacity to overcome platinum resistance in XRCC1-deficient epithelial ovarian cancers [38] and

selectively eliminate BRCA2-deficient cells [39]. Clinically, low MRN complex expression in resected gastric cancer specimens correlates with robust responses to cisplatin chemotherapy [40]. It has also been reported that disruption of the MRN complex or its components can render cancer cells sensitive to cisplatin, increasing DNA damage and cell death [41, 42]. Conversely, MRE11 overexpression is frequently associated with chemoresistance across various malignancies [17, 43]. Given the prominent role of MRE11 in DNA repair, we investigated whether its pharmacological inhibition via the small-molecule inhibitor mirin could link cisplatin- and radiation-induced damage to enhance radiosensitivity in NSCLC cell lines. Mirin reduced the clonogenic survival of NSCLC cells in a time- and dose-dependent manner, an effect that was further potentiated when combined with cisplatin. Crucially, with the exception of H1975, the CP-resistant lines (A549, H1299, H838, H520, and H23) exhibited a profound decline in clonogenic survival following mirin monotherapy or in combination with CP. Strikingly, triple combination therapy (mirin + CP + IR) further suppressed the surviving fraction, though this synergism was restricted to a subset of the CP-resistant panel (A549, H838, and H520). To elucidate the underlying mechanism of this combined treatment, we evaluated the impact of MRE11 inhibition on Pt-GpG crosslink kinetics. While mirin did not alter CP-adduct levels in inherently sensitive lines (H460, H661, and H522), it significantly elevated adduct accumulation in the CP resistant phenotypes (A549, H1299, H838, H520, and H23), again with the exception of H1975. This accumulation of unrepaired adducts directly mirrors the clonogenic survival deficits, reinforcing MRE11 inhibition as a promising therapeutic strategy to overcome resistance in lung carcinomas, particularly in platinum-refractory tumors.

MRE11 Inhibition Selectively Disrupts Downstream DSB Repair Signaling

Furthermore, we evaluated the impact of this combination therapy on DSB repair signaling pathways, given the established role of the MRN complex in sensing and processing DSBs via HRR and NHEJ [16]. Because MRE11 facilitates DNA end resection, a critical commitment step that promotes HRR over NHEJ, the formation of 53BP1 and RAD51 foci was quantified as surrogate markers for NHEJ and HRR activity, respectively. Notably, 53BP1 was selected over γH2AX because it serves as a highly

conserved checkpoint sensor that directly regulates DSB repair pathway choice [44]. Our data demonstrate that combining mirin and cisplatin significantly impairs the initial formation of radiation-induced 53BP1 foci. Strikingly, this inhibition was restricted to the CP-resistant cohort (A549, H1299, H838, H520, and H23), with the sole exception of H1975, while leaving CP-sensitive lines unaffected. In contrast, the combination significantly suppressed initial RAD51 foci formation across nearly the entire panel, sparing only the H661 cell line. These observations reveal that mirin potently synergizes with CP to disrupt HRR signaling globally, whereas it selectively compromises 53BP1-dependent repair pathways in a predominantly platinum-resistant background. Crucially, this dual inhibition occurs at a low, clinically relevant cisplatin concentration (2 μM), which closely mirrors the established patient plasma range of 3–6 μM (1–2 mg/L).

Tumor-Specific Selectivity and Safety Profile in Normal Fibroblasts

In the final part of this study, neonatal and adult human dermal fibroblasts (HDFN and HDFA) were utilized as non-transformed cellular models to determine whether the observed radiosensitization and repair disruption were tumor-specific. Our investigation revealed that neither mirin nor its combination with cisplatin (CP) significantly altered the radiosensitivity of these normal fibroblasts; rather, a modest increase in the surviving fraction was observed. Regarding platinum kinetics, both fibroblast cultures demonstrated that proliferation rates dictate adduct dynamics: exponentially growing cells with high proliferation rates rapidly accumulated CP adducts within four hours, followed by a swift decline. Conversely, plateau-phase cells with low proliferation rates accumulated adducts more slowly, peaking at approximately 12 hours before undergoing a gradual reduction.

To further characterize the impact of CP on normal tissue models, it is worth noting that the combined effect of cisplatin and ionizing radiation on apoptotic cell death of peripheral blood lymphocytes was found to be strictly additive [45]. Crucially, this additive toxicity was entirely independent of the proliferation status of the lymphocytes, manifesting consistently in both resting G0 and proliferating cells PBMCs [45]. This discrepancy likely reflects cell type-specific survival strategies: while structural cells like fibroblasts rely on active, proliferation-linked metabolic and repair pathways to process DNA lesions, lymphocytes are highly primed for p53-mediated apoptosis, where transcription stress

from cisplatin adducts combined with radiation-induced strand breaks triggers cell death irrespective of replication.

Intriguingly, mirin treatment significantly decreased CP-adduct formation across all experimental groups in both fibroblast lines, suggesting that MRE11 inhibition exerts a paradoxical protective effect against adduct accumulation in non-transformed cells. This phenomenon provides a plausible mechanistic explanation for the slight increase in fibroblast survival following 2 Gy irradiation. In stark contrast, none of the NSCLC cell lines exhibited a decrease in CP-adduct formation upon mirin treatment, strongly underscoring the tumor-specific selectivity of this approach. Furthermore, no substantial alterations were detected in the initial formation of γH2AX, 53BP1, or RAD51 foci in any fibroblast treatment group, indicating that their DNA damage response (DDR) signaling remains functionally intact. These findings align with the established paradigm that normal cells possess greater DDR redundancy and metabolic adaptability than cancer cells, thereby minimizing the risk of off-target clinical toxicity [46, 47].

Conclusion and Future Perspectives

In summary, this study demonstrates that MRE11 inhibition via mirin effectively radiosensitizes platinum-resistant NSCLC cells during combined cisplatin and ionizing radiation treatment. Preclinically, these findings align with evidence that MRE11 depletion, via genetic knockdown or pharmacological blockade, reverses cisplatin resistance in ovarian cancer cells and 3D spheroid models [47]. Clinically, an analysis of the randomized CALGB 89803 trial [48] in stage III colon cancer patients revealed that MRE11 deficiency correlates with improved long-term disease-free and overall survival, serving as a favorable prognostic marker independent of treatment. Validating these findings in larger, independent cohorts could establish MRE11 as a robust clinical biomarker. Consequently, mirin provides a valuable proof-of-concept for integrating MRE11 inhibitors into standard first-line chemo-radiotherapy regimens for locally advanced lung cancer. Ultimately, targeting the MRN complex represents a viable strategy to overcome platinum resistance and induce tumor-specific synthetic lethality. To advance this approach clinically, novel MRE11 inhibitors such as MU147 and

MU1409, which possess significantly higher potency than mirin [49], should be evaluated in future translational studies combining cisplatin and radiotherapy.

Declarations

Abbreviations

CP: cisplatin; **NSCLC**: non-small cell lung cancer; **IR**: ionizing radiation; **DSB**: DNA double-strand break; **DDR**: DNA damage response; **MRN**: MRE11-RAD50-NBS1; **ATM**: ataxia-telangiectasia-mutated; **HRR**: homologous recombination repair; **NHEJ**: non-homologous end joining; **HDFN**: human dermal fibroblast neonatal; **HDFA**: human dermal fibroblast adult.

Ethics approval and consent to participate: not applicable

Consent for publication: not applicable

Availability of data and materials: The datasets used and/or analyzed during the current study are available from the corresponding author on reasonable request.

Competing Interest: The authors declare that they have no competing interests.

Funding: This work was supported by the German Federal Ministry of Education and Research (BMBF) within the "Collar" project under grant number 02NUK043B.

Author Contributions: Conceptualization, A.S., E.B.Y., J.T., G.I., M.G. and M.S.; methodology, A.S., E.B.Y., J.T. and G.I.; resources, A.S., M.G. and M.S.; data curation, E.B.Y., A.S., M.G. and M.S.; writing, E.B.Y. and A.S.; project administration, A.S., G.I., M.G. and M.S. All authors have read and agreed to the published version of the manuscript.

Acknowledgements: The authors would like to thank Michael Groneberg/[1]Department of Radiation Therapy, University Hospital Essen for his technical support with cell culture and microscopy.

References

1. Siegel RL, Miller KD, Wagle NS, Jemal A. Cancer statistics, 2023. CA Cancer J Clin. 2023;73:17-48. doi: 10.3322/caac.21763.

2. Planchard D, Popat S, Kerr K, Novello S, Smit EF, Faivre-Finn C, Mok TS, Reck M, Van Schil PE, Hellmann MD, Peters S. Metastatic non-small cell lung cancer: ESMO Clinical Practice Guidelines for diagnosis, treatment and follow-up. Ann Oncol. 2018; 29:iv192-iv237. doi: 10.1093/annonc/mdy275.

3. Chen SH and Chang JY. New insights into mechanisms of cisplatin resistance: from tumor cell to microenvironment. Int J Mol Sci. 2019; 20: 4136. doi: 10.3390/ijms20174136.

4. Stewart DJ. Mechanisms of resistance to cisplatin and carboplatin. Crit Rev Oncol Hematol. 2007;63:12-31. doi: 10.1016/j.critrevonc.2007.02.001.

5. Siddik ZH. Cisplatin: mode of cytotoxic action and molecular basis of resistance. Oncogene. 2003;22:7265-79. doi: 10.1038/sj.onc.1206933.

6. Wang D and Lippard SJ. Cellular processing of platinum anticancer drugs. Nat Rev Drug Discov. 2005; 4:307-20. doi: 10.1038/nrd1691.

7. Zeman MK and Cimprich KA. Causes and consequences of replication stress. Nat Cell Biol. 2014;16: 2-9. doi: 10.1038/ncb2897.

8. Galluzzi L, Senovilla L, Vitale I, Michels J, Martins I, Kepp O, Castedo M, Kroemer G. Molecular mechanisms of cisplatin resistance. Oncogene. 2012;31:1869-83. doi: 10.1038/onc.2011.384.

9. Shtivelman E, Hensing T, Simon GR, Dennis PA, Otterson GA, Bueno R, Salgia R. Molecular pathways and therapeutic targets in lung cancer. Oncotarget. 2014;5:1392-433. doi: 10.18632/oncotarget.1891.
10. Brabec V and Kasparkova J. Molecular aspects of resistance to antitumor platinum drugs. Drug Resist Updat. 2002;5:147-61. doi: 10.1016/s1368-7646(02)00047-x.

11. Martin LP, Hamilton TC, Schilder RJ. Platinum resistance: the role of DNA repair pathways. Clin Cancer Res. 2008;14:1291-5. doi: 10.1158/1078-0432.CCR-07-2238.

12. Amable L. Cisplatin resistance and opportunities for precision medicine. Pharmacol Res. 2016;106:27-36. doi: 10.1016/j.phrs.2016.01.001.

13. Mavragani IV, Nikitaki Z, Souli MP, Aziz A, Nowsheen S, Aziz K, Rogakou E, Georgakilas AG. Complex DNA damage: a route to radiation-induced genomic instability and carcinogenesis. Cancers (Basel). 2019;11:1789. doi: 10.3390/cancers11111789.

14. Kastan MB and Lim DS. The many substrates and functions of ATM. Nat Rev Mol Cell Biol. 2000;1:179-86. doi: 10.1038/35043058.

15. Kastan MB. Checking two steps. Nature. 2001; 410:766-7. doi: 10.1038/35071218.

16. Stracker TH and Petrini JH. The MRE11 complex: starting from the ends. Nat Rev Mol Cell Biol. 2011;12:90-103. doi: 10.1038/nrm3047.

17. Dupré A, Boyer-Chatenet L, Sattler RM, Modi AP; Lee JH; Nicolette ML, Kopelovich L, Jasin M, Baer R, Paull TT, Gautier J. A forward chemical genetic screen reveals an inhibitor of the Mre11–Rad50–Nbs1 complex. Nat Chem Biol. 2008;4:119-25. doi: 10.1038/nchembio.63.

18. Shibata A, Moiani D, Arvai AS, Perry J, Harding SM, Genois MM, Maity R, van Rossum-Fikkert S, Kertokalio A, Romoli F, Ismail A, Ismalaj E, Petricci E, Neale MJ, Bristow RG, Masson JY, Wyman C, Jeggo PA, Tainer JA. DNA double-strand break repair pathway choice is directed by distinct MRE11 nuclease activities. Mol Cell. 2014;53:7-18. doi: 10.1016/j.molcel.2013.11.003.

19. Gerina-Berzina A, Hasnere S, Kolesovs A, Umbrashko S, Muceniece R, Nakurte I. Determination of cisplatin in human blood plasma and urine using liquid chromatography-mass spectrometry for oncological patients with a variety of fatty tissue mass for prediction of toxicity. Exp Oncol. 2017;39:124-130.

20. Rajkumar P, Mathew BS, Das S, Isaiah R, John S, Prabha R, Fleming DH. Cisplatin concentrations in long and short duration infusion: implications for the optimal time of radiation delivery. J Clin Diagn Res. 2016;10:XC01-XC04. doi: 10.7860/JCDR/2016/18181.8126.

21. Qiu Y, Lin X, Mladenov E, Mladenova V, Thomale J, Sak A, Wang Y, Deng Y, Gkika E, Stuschke M, Iliakis G. Cell-cycle-specific lesion evolution rather than inhibition of double-strand-break repair underpins cisplatin radiosensitization. Mol Oncol. 2026;20:1814-34. doi: 10.1002/1878-0261.70240.

22. Wang LH, Li Y, Yang SN, Wang FY, Hou Y, Cui W, Chen K, Cao Q, Wang S, Zhang TY, Wang ZZ, Xiao W, Yang JY, Wu CF. Gambogic acid synergistically potentiates cisplatin-induced apoptosis in non-small-cell lung cancer through suppressing NF-κB and MAPK/HO-1 signalling. Br J Cancer. 2014;110:341-52. doi: 10.1038/bjc.2013.752.

23. Almeida GM, Duarte TL, Farmer PB, Steward WP, Jones GD. Multiple end-point analysis reveals cisplatin damage tolerance to be a chemoresistance mechanism in a NSCLC model: Implications for predictive testing. Int J Cancer. 2008;122:1810-9. doi: 10.1002/ijc.23188.

24. Van Schaeybroeck S, Kyula J, Kelly DM, Karaiskou-McCaul A, Stokesberry SA, Van Cutsem E, Longley DB, Johnston PG. Chemotherapy-induced epidermal growth factor receptor activation determines response to combined gefitinib/chemotherapy treatment in non–small cell lung cancer cells. Mol Cancer Ther. 2006;5:1154-65. doi: 10.1158/1535-7163.MCT-05-0446.

25. Lundholm L, Hååg P, Zong D, Juntti T, Mörk B, Lewensohn R, Viktorsson K. Resistance to DNA-damaging treatment in non-small cell lung cancer tumor-initiating cells involves reduced DNA-PK/ATM activation and diminished cell cycle arrest. Cell Death Dis. 2013;4: e478. doi: 10.1038/cddis.2012.211.

26. Lemaire MA, Schwartz A, Rahmouni AR, Leng M. Interstrand cross-links are preferentially formed at the d (GC) sites in the reaction between cis-diamminedichloroplatinum (II) and DNA. Proc Natl Acad Sci U S A. 1991;88:1982-5. doi: 10.1073/pnas.88.5.1982.

27. Köberle B, Grimaldi KA, Sunters A, Hartley JA, Kelland LR, Masters JR. DNA repair capacity and cisplatin sensitivity of human testis tumour cells. Int J Cancer 1997;70:551-5. doi: 10.1002/(sici)1097-215(19970304)70:5<551::aid-ijc10>3.0.co;2-g.

28. Shellard SA, Hosking LK, Hill BT. Anomalous relationship between cisplatin sensitivity and the formation and removal of platinum-DNA adducts in two human ovarian carcinoma cell lines in vitro. Cancer Res. 1991;51:4557-64.

29. Gupta S, Koru-Sengul T, Arnold SM, Devi GR, Mohiuddin M, Ahmed MM. Low-dose fractionated radiation potentiates the effects of cisplatin independent of the hyper-radiation sensitivity in human lung cancer cells. Mol Cancer Ther. 2011;10:292-302. doi: 10.1158/1535-7163.MCT-10-0630.

30. Toulany M, Mihatsch J, Holler M, Chaachouay H, Rodemann HP. Cisplatin-mediated radiosensitization of non-small cell lung cancer cells is stimulated by ATM inhibition. Radiother Oncol. 2014;111:228-36. doi: 10.1016/j.radonc.2014.04.001.

31. da Silva GN, de Camargo EA, Sávio AL, Salvadori DM. MRE11A and SKP2 genes are associated with the increased cytotoxicity induced by the synergistic effects of cisplatin and gemcitabine in bladder cancer cells. Mol Biol Rep. 2014;41:4613-21. doi: 10.1007/s11033-014-3332-1.

32. Sak A, Grehl S, Engelhard M, Wierlemann A, Kaelberlah HP, Erichsen P, Pöttgen C, Groneberg M, Stuschke M. Long-term in vivo effects of Cisplatin on γ-H2AX foci signaling in peripheral lymphocytes of tumor patients after irradiation. Clin Cancer Res. 2009;15: 2927-34. doi: 10.1158/1078-0432.CCR-08-0650.

33. Kothandapani A, Gopalakrishnan K, Kahali B, Reisman D, Patrick SM. Downregulation of SWI/SNF chromatin remodeling factor subunits modulates cisplatin cytotoxicity. Exp Cell Res**.** 2012;318:1973-86. doi: 10.1016/j.yexcr.2012.06.011.

34. Lee J and Paull TT. Activation and regulation of ATM kinase activity in response to DNA double-strand breaks. Oncogene. 2007;26:7741-8. doi: 10.1038/sj.onc.1210872.

35. Kitagawa R. and Kastan M. The ATM-dependent DNA damage signaling pathway. Cold Spring Harb Symp Quant Biol. 2005;70:99-109. doi: 10.1101/sqb.2005.70.002.

36. Schlacher K, Christ N, Siaud N, Egashira A, Wu H, Jasin M. Double-strand break repair-independent role for BRCA2 in blocking stalled replication fork degradation by MRE11. Cell. 2011;145:529-42. doi: 10.1016/j.cell.2011.03.041.

37. Du D, Yang Y, Zhang Y, Wang G, Chen L, Guan X, Rasmussen LJ, Liu D. MRE11A: a novel negative regulator of human DNA mismatch repair. Cell Mol Biol Lett. 2024;29:37. doi: 10.1186/s11658-024-00547-z.

38. Alblihy A, Ali R, Algethami M, Shoqafi A, Toss MS, Brownlie J, Tatum NJ, Hickson I, Moran PO, Grabowska A, Jeyapalan JN, Mongan NP, Rakha EA, Madhusudan S. Targeting Mre11 overcomes platinum resistance and induces synthetic lethality in XRCC1 deficient epithelial ovarian cancers. NPJ Precis Oncol. 2022; 6:51. doi: 10.1038/s41698-022-00298-0.

39. Alblihy A, Ali R, Algethami M, Ritchie AA, Shoqafi A, Alqahtani S, Mesquita KA, Toss MS, Ordóñez-Morán P, Jeyapalan JN, Dekker L, Salerno M, Hartsuiker E, Grabowska AM, Rakha EA, Mongan NP, Madhusudan S. Selective killing of BRCA2-deficient ovarian cancer cells via MRE11 blockade. Int J Mol Sci. 2023;24:10966. doi: 10.3390/ijms241310966.

40. Altan B, Yokobori T, Ide M, Bai T, Yanoma T, Kimura A, Kogure N, Suzuki M, Bao P, Mochiki E, Ogata K, Handa T, Kaira K, Nishiyama M, Asao T, Oyama T, Kuwano H. High expression of MRE11–RAD50–NBS1 is associated with poor prognosis and chemoresistance in gastric cancer. Anticancer Res. 2016;36:5237-5247. doi: 10.21873/anticanres.11094.

41. Araki K, Yamashita T, Reddy N, Wang H, Abuzeid WM, Khan K, O'Malley BW Jr, Li D. Molecular disruption of NBS1 with targeted gene delivery enhances chemosensitisation in head and neck cancer. Br J Cancer. 2010;103:1822-30. doi: 10.1038/sj.bjc.6605980.

42. Abuzeid WM, Jiang X, Shi G, Wang H, Paulson D, Araki K, Jungreis D, Carney J, O'Malley BW Jr, Li D. Molecular disruption of RAD50 sensitizes human tumor cells

to cisplatin-based chemotherapy. J Clin Invest. 2009;119:1974-85. doi: 10.1172/JCI33816.

43. Daley JM and Sung P. 53BP1, BRCA1, and the choice between recombination and end joining at DNA double-strand breaks. Mol Cell Biol. 2014;34:1380-8. doi: 10.1128/MCB.01639-13.

44. Helleday T, Petermann E, Lundin C, Hodgson B, Sharma SA. DNA repair pathways as targets for cancer therapy. Nat Rev Cancer. 2008;8:193-204. doi: 10.1038/nrc2342.

45. Sak A, Mladenov E, Alberti Y, Stuschke M. Cisplatin enhances radiation-induced apoptosis in peripheral lymphocytes of cancer patients: in vivo and in vitro findings. Radiat Oncol. 2026;21:121. doi: 10.1186/s13014-026-02921-x.

46. O'Connor MJ. Targeting the DNA damage response in cancer. Mol Cell. 2015;60:547-60. doi: 10.1016/j.molcel.2015.10.040.

47. Alblihy A, Ali R, Algethami M, Ritchie AA, Shoqafi A, Alqahtani S, Mesquita KA, Toss MS, Ordóñez-Morán P, Jeyapalan JN, Dekker L, Salerno M, Hartsuiker E, Grabowska AM, Rakha EA, Mongan NP, Madhusudan S. Selective Killing of BRCA2-Deficient Ovarian Cancer Cells via MRE11 Blockade. Int J Mol Sci. 2023;24:10966. doi: 10.3390/ijms241310966.

48. Pavelitz T, Renfro L, Foster NR, Caracol A, Welsch P, Lao VV, Grady WB, Niedzwiecki D, Saltz LB, Bertagnolli MM, Goldberg RM, Rabinovitch PS, Emond M, Monnat RJ Jr, Maizels N. MRE11-deficiency associated with improved long-term disease free survival and overall survival in a subset of stage III colon cancer patients in randomized CALGB 89803 trial. PLoS One. 2014;9:e108483. doi: 10.1371/journal.pone.0108483. eCollection 2014.

49. Nikulenkov F, Carbain B, Biswas R, Havel S, Prochazkova J, Sisakova A, Zacpalova M, Chavdarova M, Marini V, Vsiansky V, Weisova V, Slavikova K, Biradar D, Khirsariya P, Vitek M, Sedlak D, Bartunek P, Daniel L, Brezovsky J, Damborsky J, Paruch K, Krejci L. Discovery of new inhibitors of nuclease MRE11. Eur J Med Chem. 2025;285:117226. doi: 10.1016/j.ejmech.2024.117226.

Figures and Tables

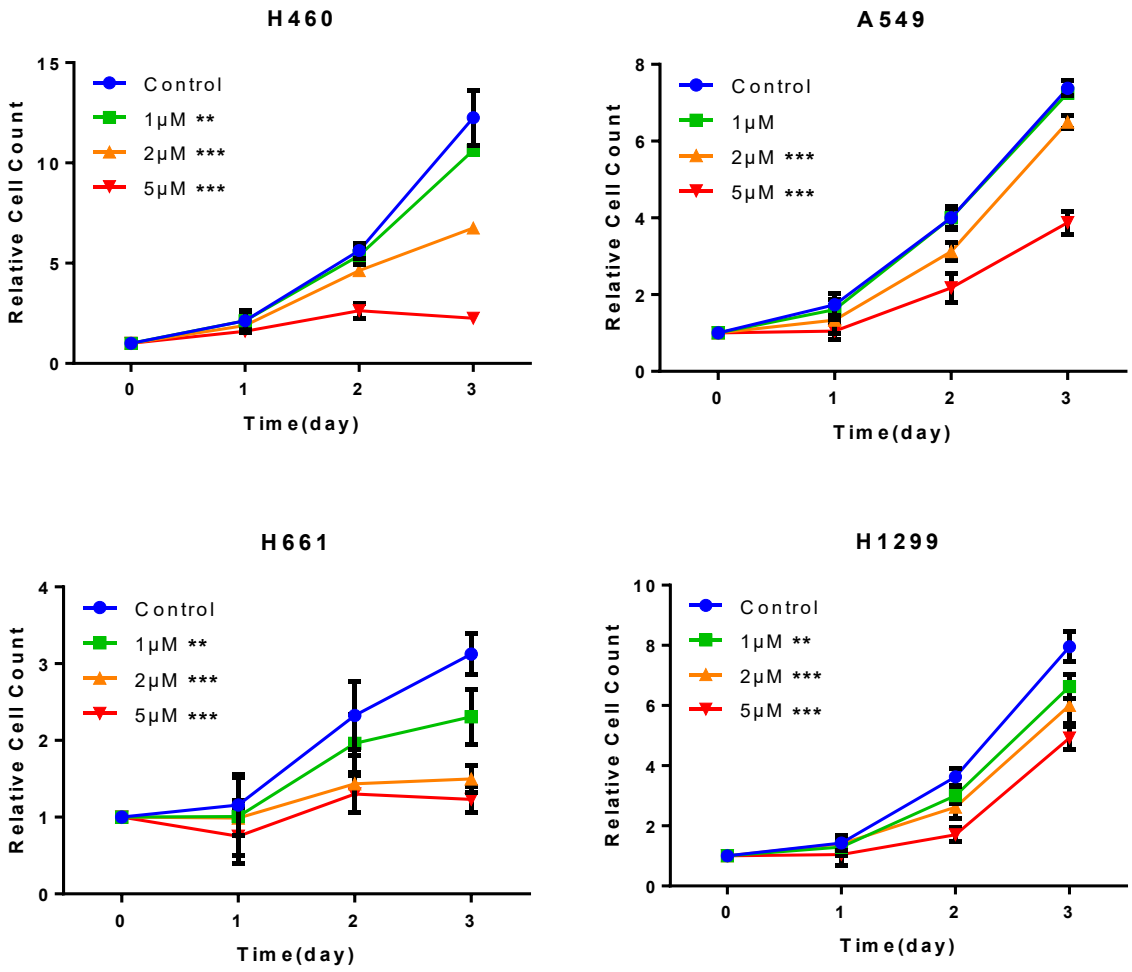
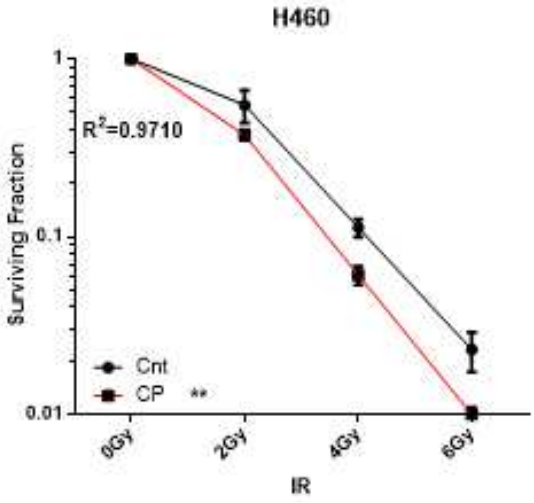
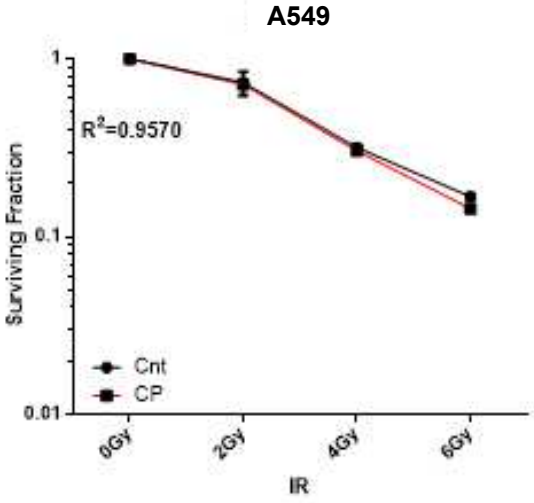


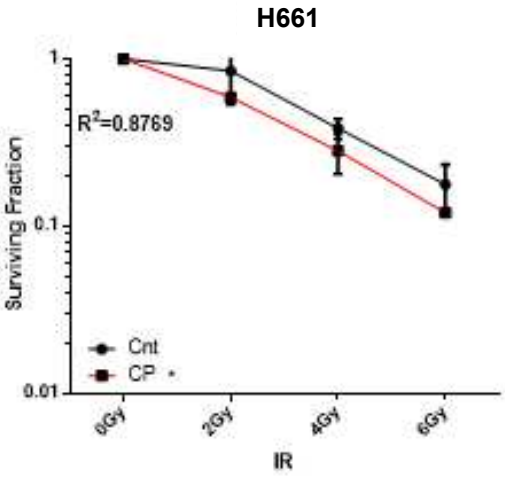
Figure 1: Effect of cisplatin on proliferation of human NSCLC cell lines. NSCLC cell lines (H460, A549, H661 and H1299) were exposed to cisplatin concentrations of 0, 1, 2 and 5 μM for four hours, and the number of cells was counted at 24, 48 and 72 hours after CP washout. The data presented herein signifies the mean ± standard deviation of three to four independent experiments. Statistically significant differences compared with corresponding control cells (not treated with cisplatin) are shown (*P < 0.05, **P < 0.01, ***P < 0.001).

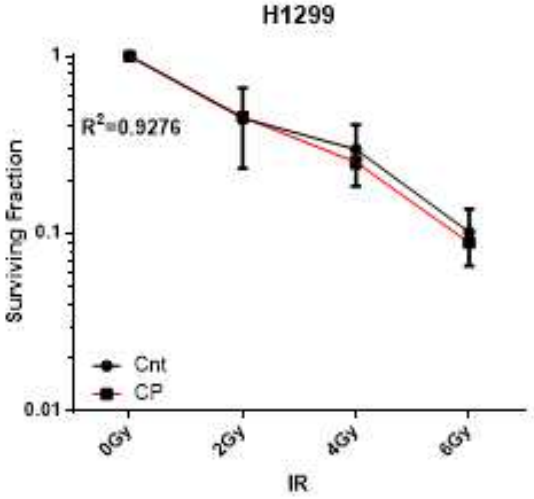
Table 1: IC50 values calculated 72 hours post-washout and their 95% confidence intervals (CI) from 3-4 experiments.

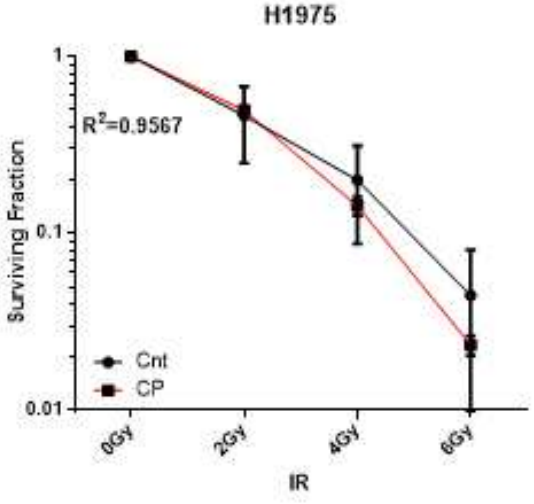
Cell Line	IC50 Value ± CI (μM)
H661	1,222 (1,001 — 1,492)
H522	1,404 (1,206 — 2,005)
H460	2,036 (1,941 — 2,135)
H838	2,559 (2,112 — 3,184)
H520	2,751 (2,480 — 2,919)
H23	2,876 (1,460 — 3,392)
H1299	3.88 (2,676 — 8,997)
H1975	3,632 (2,501 — 5,295)
A549	4,433 (3,451 — 5,693)


H460
R²=0.9710
Surviving Fraction
1
0.1
0.01
Cnt
CP **
0Gy
2Gy
4Gy
6Gy
IR


A549
R²=0.9570
Surviving Fraction
1
0.1
0.01
Cnt
CP
0Gy
2Gy
4Gy
6Gy
IR


H661
R²=0.8769
Surviving Fraction
1
0.1
0.01
Cnt
CP *
0Gy
2Gy
4Gy
6Gy
IR


H1299
R²=0.9276
Surviving Fraction
1
0.1
0.01
Cnt
CP
0Gy
2Gy
4Gy
6Gy
IR


H1975
R²=0.9567
Surviving Fraction
1
0.1
0.01
Cnt
CP
0Gy
2Gy
4Gy
6Gy
IR

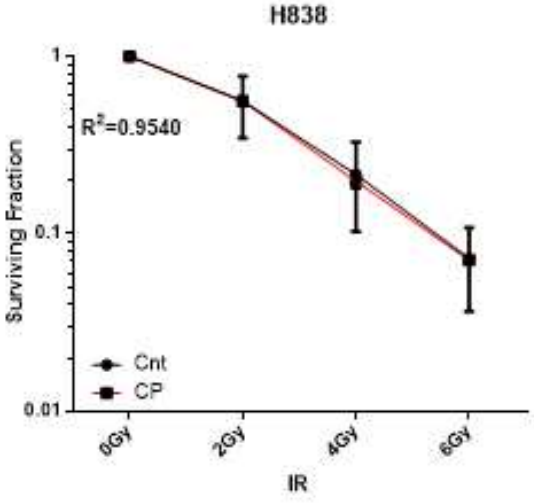

H838
R²=0.9540
Surviving Fraction
1
0.1
0.01
Cnt
CP
0Gy
2Gy
4Gy
6Gy
IR

Figure 2: Effect of Cisplatin on human NSCLC clonogenic survival. NSCLC cells were plated for clonogenic survival assays after exposure to cisplatin (2 μM) for 4h. After allowing the cells to attach, the colonies were irradiated with 0, 2, 4 and 6 Gy and left for incubation for 10 - 18 days. Data represents mean ± SD of 3–4 independent experiments. Statistically significant differences compared with corresponding control cells (not treated with cisplatin) using nonlinear regression (curve fit) and globally shared R2 values are shown (*P < 0.05, **P < 0.01).

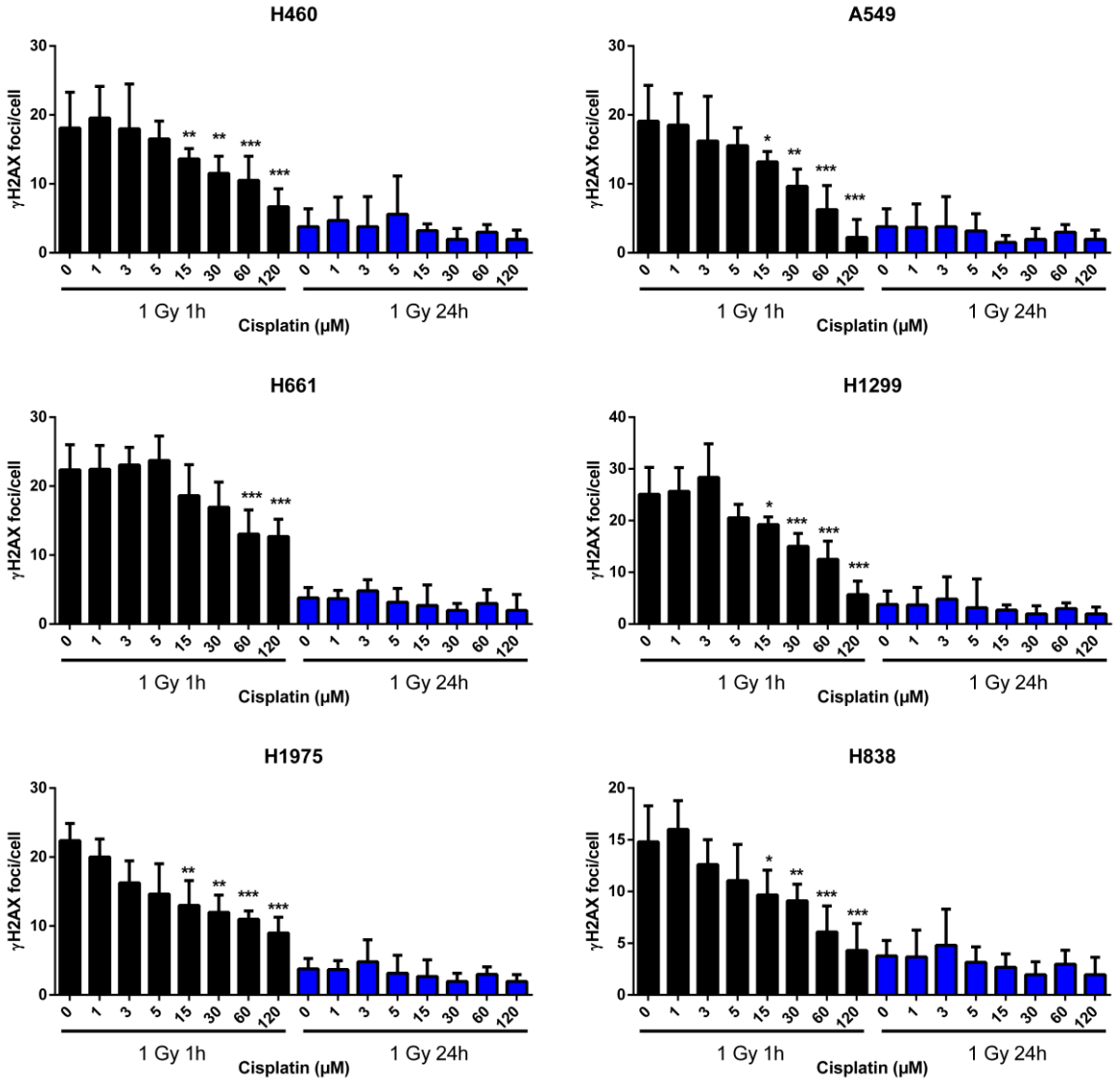
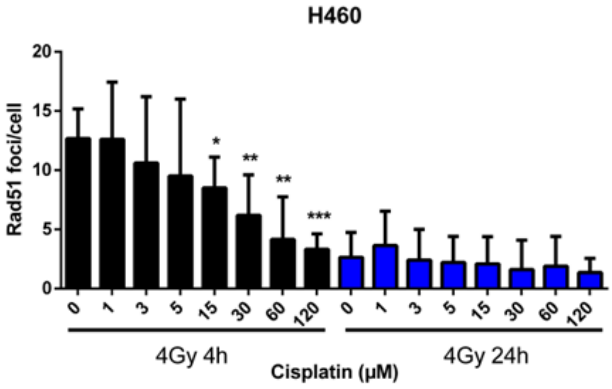
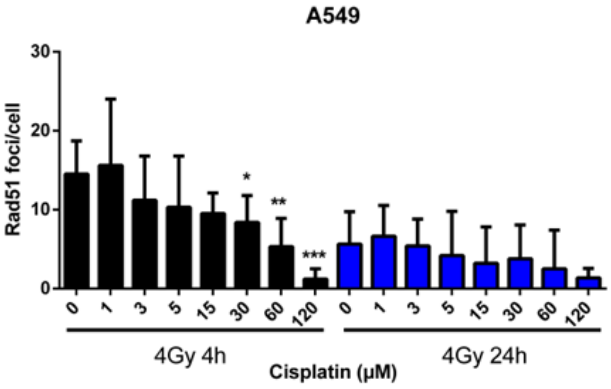
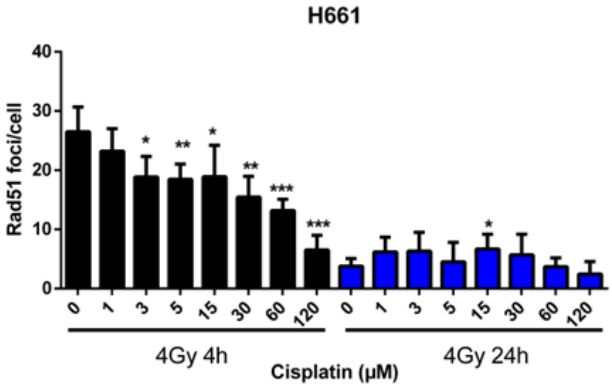
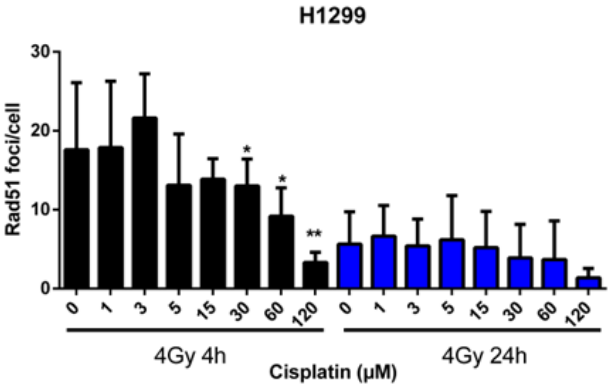


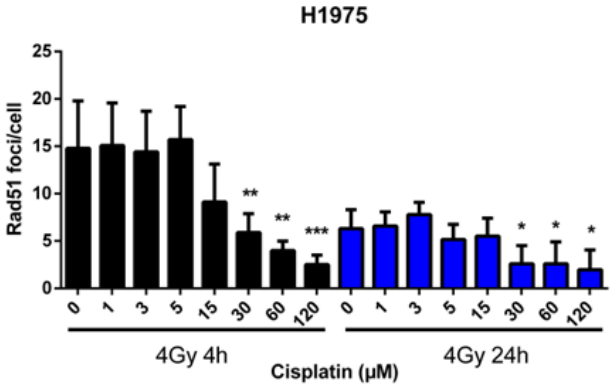
Figure 3: Effect of Cisplatin on NHEJ repair signalling of NSCLCs. Cells plated for immunofluorescence assays after exposure to cisplatin (1 to 120 μM), were irradiated with 0 Gy and 1 Gy followed by fixations at 1 h, 4 h and 24 h and γH2AX foci were scored. Data represents mean ± SD of 3–4 independent experiments are shown. Statistically significant differences compared with corresponding control cells (not treated with cisplatin) using student's t test are shown (*P < 0.05, **P < 0.01, ***P < 0.001).


H460
Rad51 foci/cell
20
15
10
5
0
*
**
**
***
0 1 3 5 15 30 60 120 0 1 3 5 15 30 60 120
4Gy 4h
4Gy 24h
Cisplatin (μM)


A549
Rad51 foci/cell
30
20
10
0
*
**
***
0 1 3 5 15 30 60 120 0 1 3 5 15 30 60 120
4Gy 4h
4Gy 24h
Cisplatin (μM)


H661
Rad51 foci/cell
40
30
20
10
0
*
**
*
**
***
***
*
0 1 3 5 15 30 60 120 0 1 3 5 15 30 60 120
4Gy 4h
4Gy 24h
Cisplatin (μM)


H1299
Rad51 foci/cell
30
20
10
0
*
*
**
0 1 3 5 15 30 60 120 0 1 3 5 15 30 60 120
4Gy 4h
4Gy 24h
Cisplatin (μM)


H1975
Rad51 foci/cell
25
20
15
10
5
0
**
**
***
*
*
*
0 1 3 5 15 30 60 120 0 1 3 5 15 30 60 120
4Gy 4h
4Gy 24h
Cisplatin (μM)

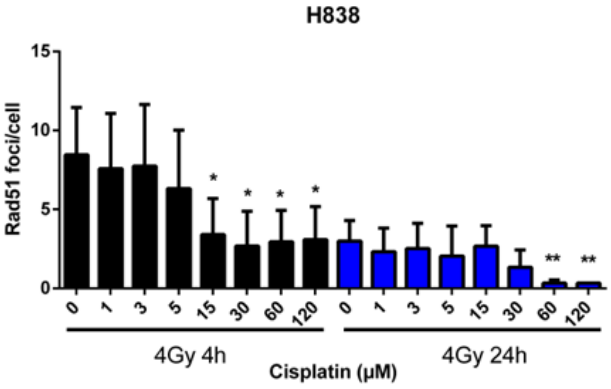

H838
Rad51 foci/cell
15
10
5
0
*
*
*
*
**
**
0 1 3 5 15 30 60 120 0 1 3 5 15 30 60 120
4Gy 4h
4Gy 24h
Cisplatin (μM)

Figure 4: Effect of cisplatin on HR repair of NSCLCs. After exposure to cisplatin (1 to 120 μM), cells were plated for immunofluorescence assays, irradiated with 0 Gy and 4 Gy followed by fixations at various times thereafter (1 h, 4 h and 24 h) and RAD51 foci were scored. The data represents mean ± SD of 3–4 independent experiments. Statistically significant differences compared with corresponding control cells (not treated with cisplatin) using student's t test are shown (*P < 0.05, **P < 0.01, ***P < 0.001).

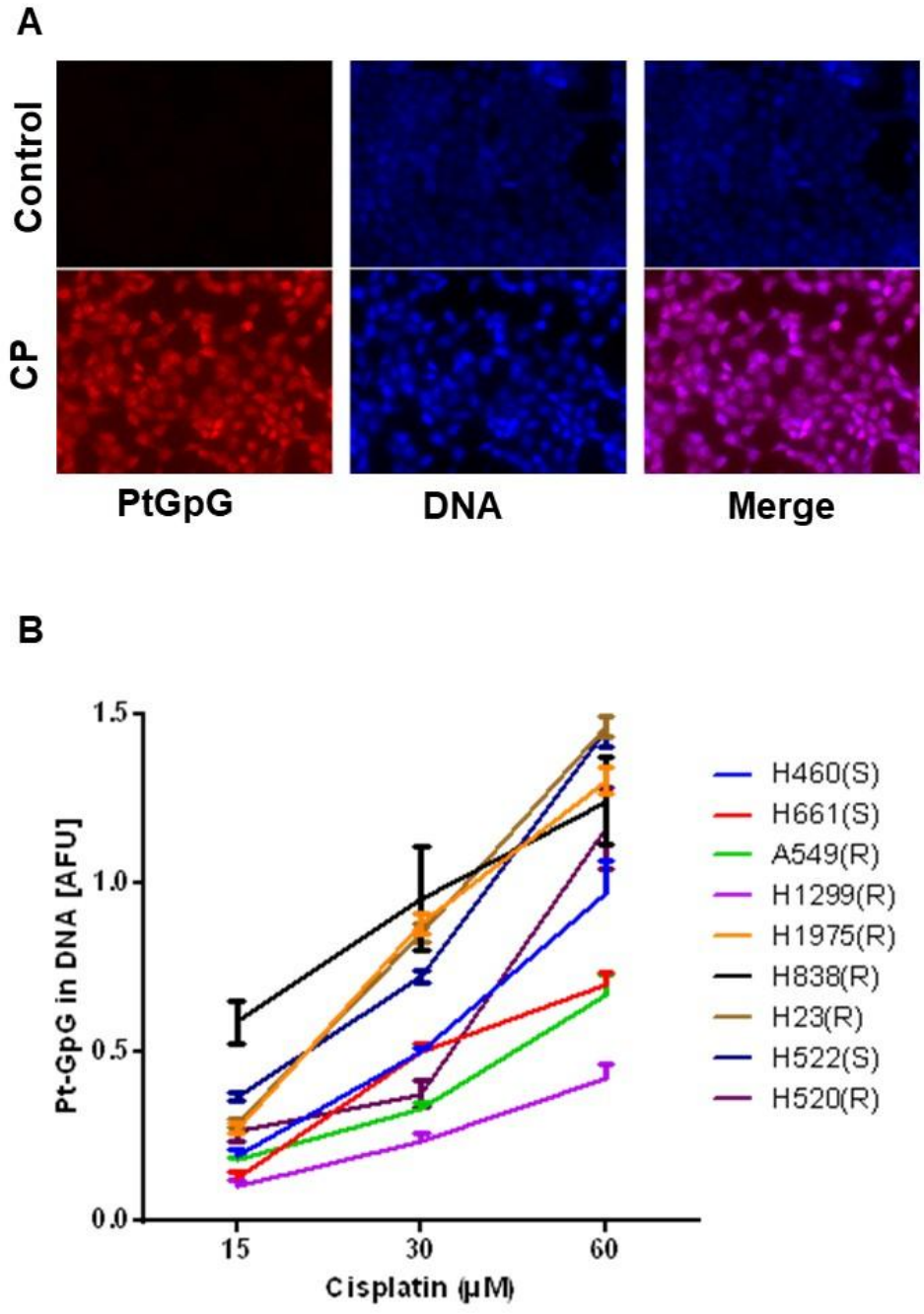
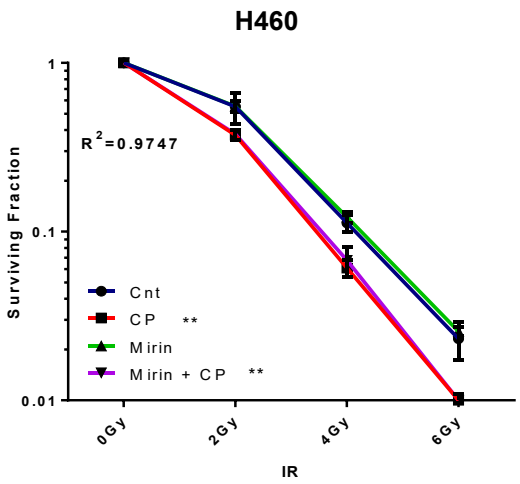
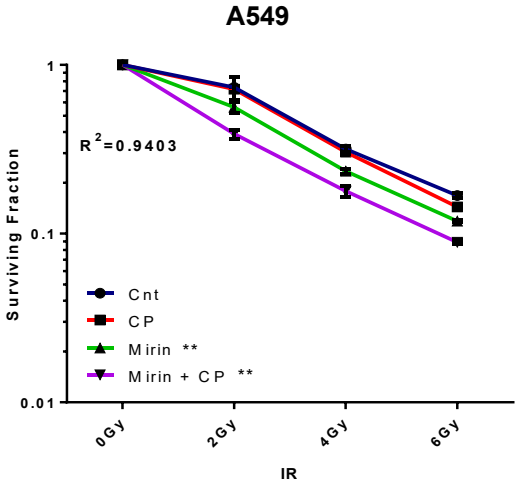
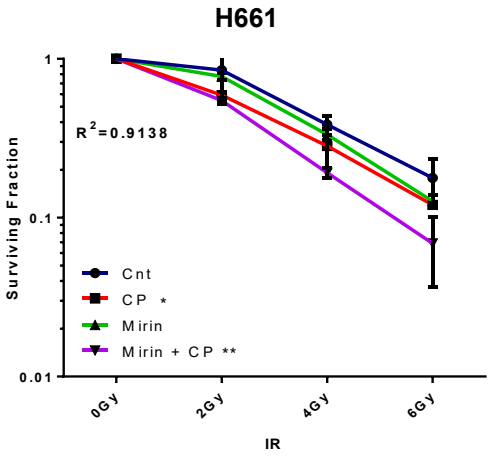
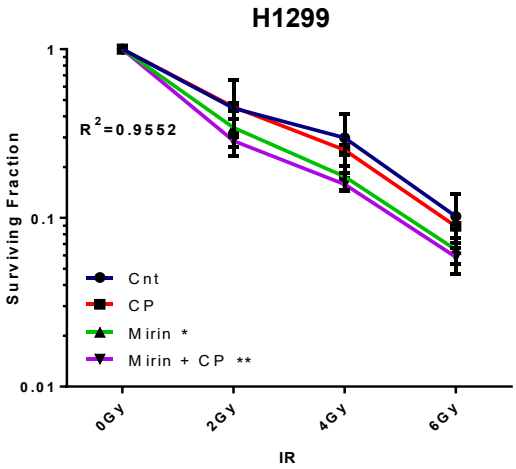


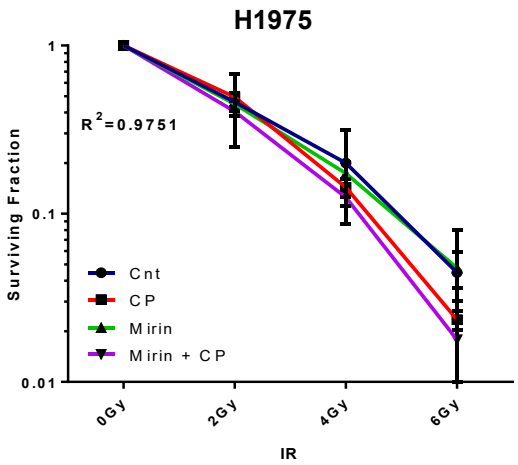
Figure 5: Formation of Pt-GpG Adducts in NSCLCs. A: Images of control and treatment (60 μM CP, 4 h) groups of the H460 cell line under fluorescence microscope. B: Pt-GpG adduct formation at 24 h after treatment with 15, 30, 60 μM Cisplatin for 4 h. Data represents mean ± SEM of 3 to independent experiments.


H460
Surviving Fraction
1
0.1
0.01
R²=0.9747
Cnt
CP **
Mirin
Mirin + CP **
0Gy
2Gy
4Gy
6Gy
IR


A549
Surviving Fraction
1
0.1
0.01
R²=0.9403
Cnt
CP
Mirin **
Mirin + CP **
0Gy
2Gy
4Gy
6Gy
IR


H661
Surviving Fraction
1
0.1
0.01
R²=0.9138
Cnt
CP *
Mirin
Mirin + CP **
0Gy
2Gy
4Gy
6Gy
IR


H1299
Surviving Fraction
1
0.1
0.01
R²=0.9552
Cnt
CP
Mirin *
Mirin + CP **
0Gy
2Gy
4Gy
6Gy
IR


H1975
Surviving Fraction
1
0.1
0.01
R²=0.9751
Cnt
CP
Mirin
Mirin + CP
0Gy
2Gy
4Gy
6Gy
IR

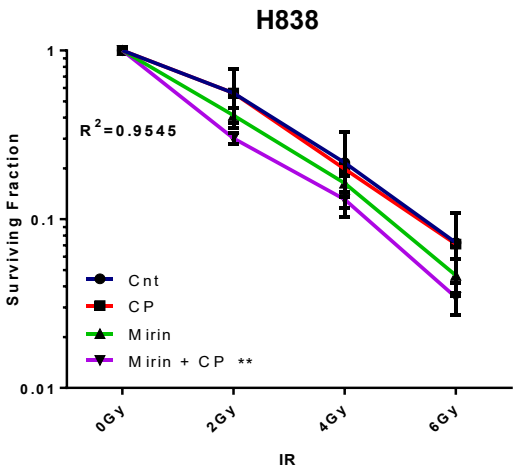

H838
Surviving Fraction
1
0.1
0.01
R²=0.9545
Cnt
CP
Mirin
Mirin + CP **
0Gy
2Gy
4Gy
6Gy
IR

Figure 6: Effect of cisplatin, mirin, and combined treatment on human NSCLC radiation sensitivity. NSCLC cell lines were treated with 20 μM mirin for 20 h followed by 2 μM cisplatin treatment for 4 h plated for clonogenic survival assays into mirin containing media for further 24 h Mirin treatment. After allowing the cells to attach for 4-5 h, the colonies were irradiated with 0, 2, 4, 6 Gy and left for incubation with mirin containing media for 24 h. The media was replaced next day and colonies were left for incubation for 10-18 days. Mean ± SD of 3–5 independent experiments are shown. Statistically significant differences compared with corresponding control cells (not treated with cisplatin) using non-linear regression (curve fit) and globally shared R2 values are shown (*P < 0.05, **P < 0.01, ***P < 0.001).

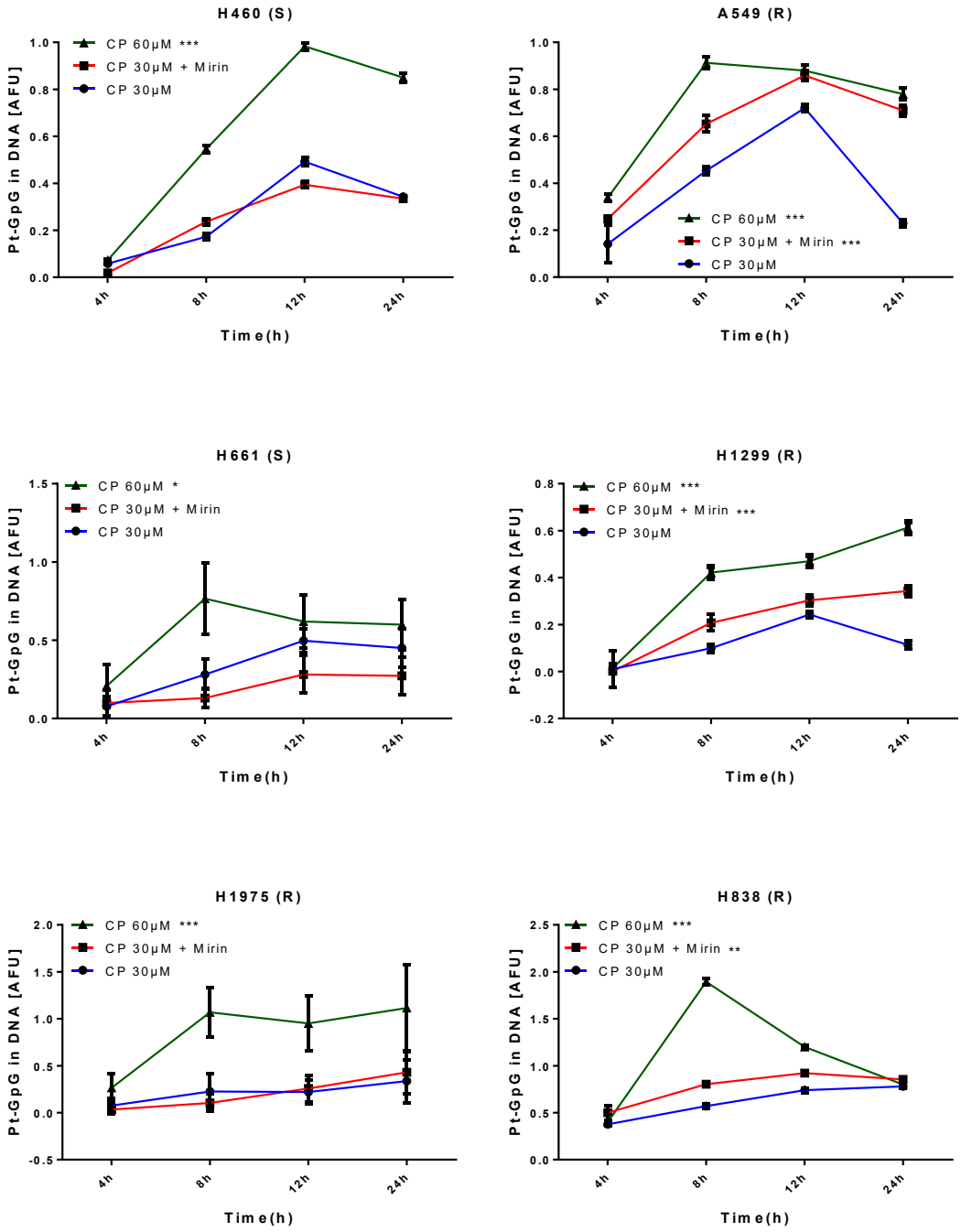
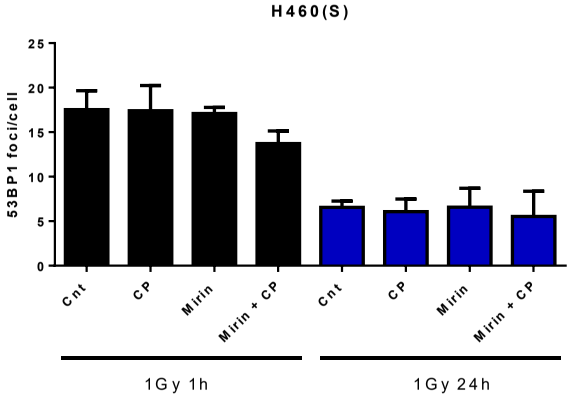
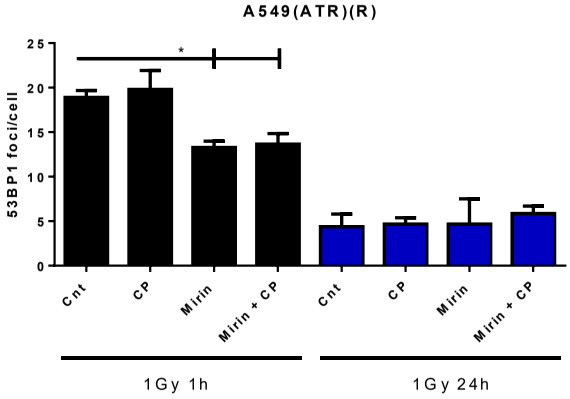
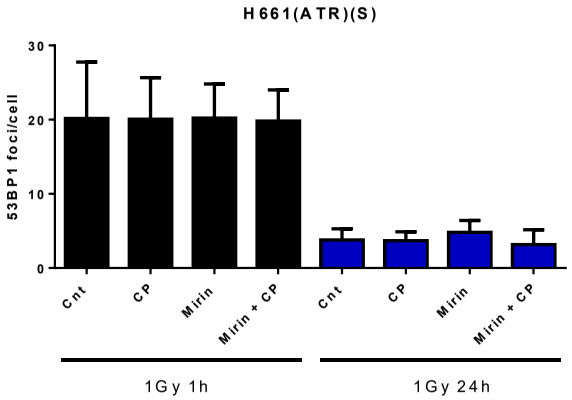
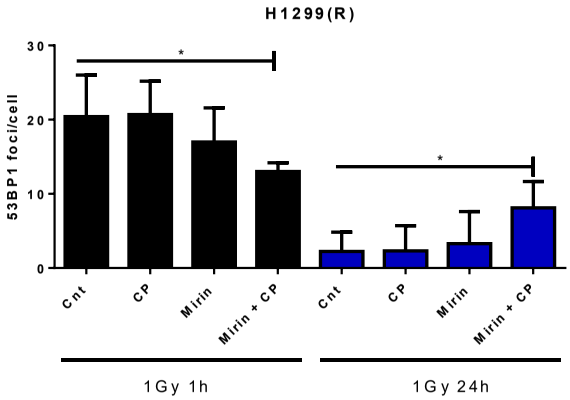


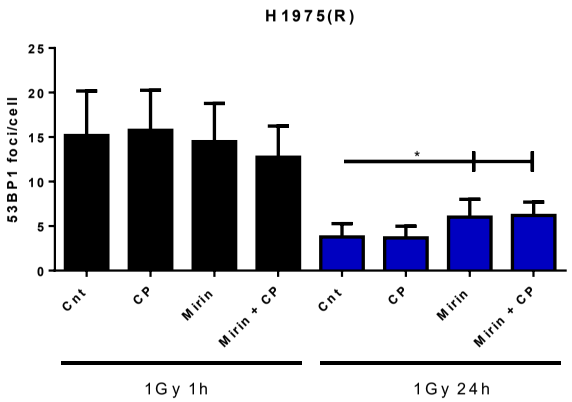
Figure 7: CP-DNA adduct kinetics after Cisplatin and Combined treatment in NSCLCs. Human NSCLC cell lines were plated for immunofluorescence assays and were treated with 20 μM Mirin for 20 h followed by 30 μM and 60 μM cisplatin treatment for 4h and fixed at 4, 8, 12 and 24h. S and R denotes cisplatin sensitive and resistant, respectively. Mean ± SD of 3–4 independent experiments are shown. Statistically significant differences compared with CP 30 μM are shown (*P < 0.05, **P < 0.01, ***P < 0.001, n=3).


H460(S)
53BP1 foci/cell
25
20
15
10
5
0
Cnt
CP
Mirin
Mirin + CP
Cnt
CP
Mirin
Mirin + CP
1Gy 1h
1Gy 24h


A549(ATR)(R)
53BP1 foci/cell
25
20
15
10
5
0
*
Cnt
CP
Mirin
Mirin + CP
Cnt
CP
Mirin
Mirin + CP
1Gy 1h
1Gy 24h


H661(ATR)(S)
53BP1 foci/cell
30
20
10
0
Cnt
CP
Mirin
Mirin + CP
Cnt
CP
Mirin
Mirin + CP
1Gy 1h
1Gy 24h


H1299(R)
53BP1 foci/cell
30
20
10
0
*
*
Cnt
CP
Mirin
Mirin + CP
Cnt
CP
Mirin
Mirin + CP
1Gy 1h
1Gy 24h


H1975(R)
53BP1 foci/cell
25
20
15
10
5
0
*
Cnt
CP
Mirin
Mirin + CP
Cnt
CP
Mirin
Mirin + CP
1Gy 1h
1Gy 24h

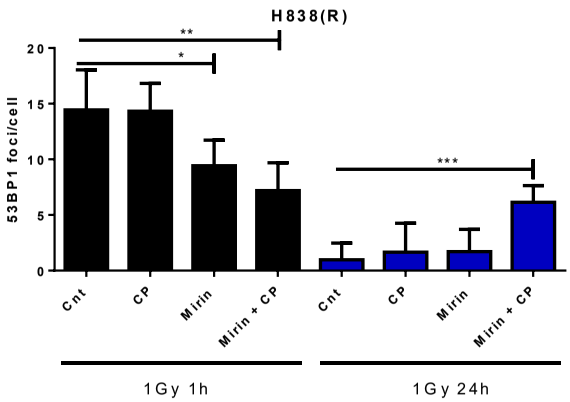
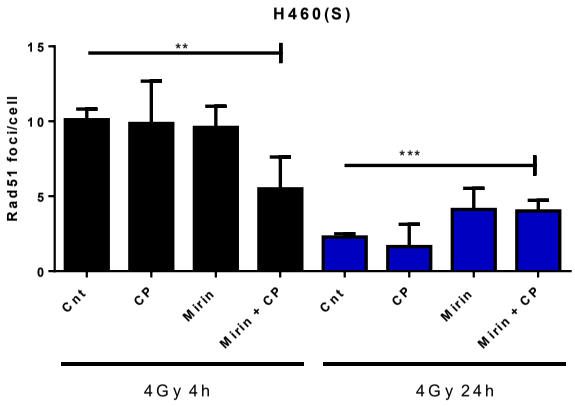
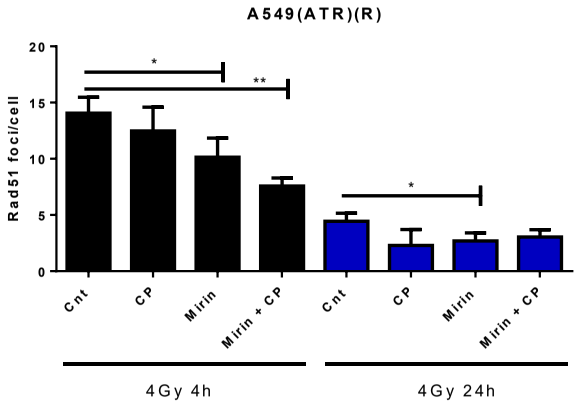
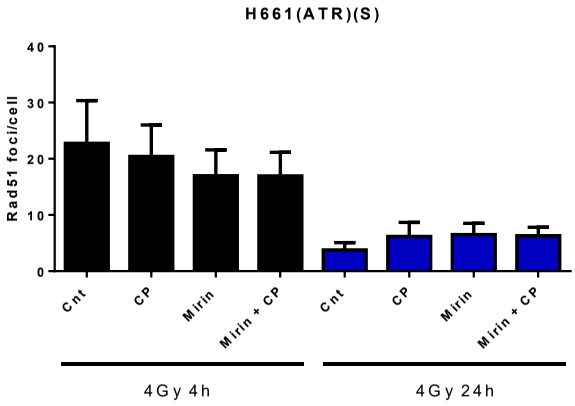
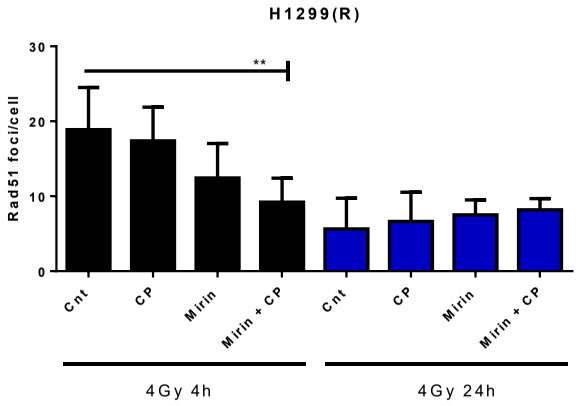

H838(R)
53BP1 foci/cell
20
15
10
5
0
**
*
***
Cnt
CP
Mirin
Mirin + CP
Cnt
CP
Mirin
Mirin + CP
1Gy 1h
1Gy 24h

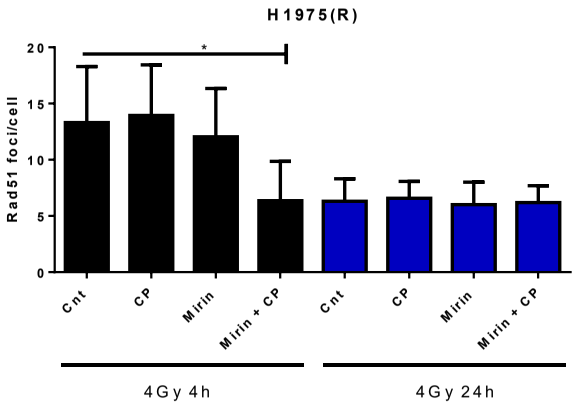
Figure 8: Effect of cisplatin, mirin and combined treatment on 53BP1 repair signalling. Human NSCLC cells were plated for immunofluorescence assays and were treated with 20 μM Mirin for 20 h followed by 2 μM cisplatin treatment for 4h and were irradiated with 0, 1 Gy prior to fixation at 1 h and 24 h, and 53BP1 foci were scored. Mean ± SD of 3–4 independent experiments are shown. Statistically significant differences compared with corresponding control cells (not treated with Cisplatin) using student's t test are shown (*P < 0.05, **P < 0.01, ***P < 0.001).


H460(S)
Rad51 foci/cell
15
10
5
0
**
***
Cnt
CP
Mirin
Mirin + CP
4Gy 4h
4Gy 24h


A549(ATR)(R)
Rad51 foci/cell
20
15
10
5
0
*
**
*
Cnt
CP
Mirin
Mirin + CP
4Gy 4h
4Gy 24h


H661(ATR)(S)
Rad51 foci/cell
40
30
20
10
0
Cnt
CP
Mirin
Mirin + CP
4Gy 4h
4Gy 24h


H1299(R)
Rad51 foci/cell
30
20
10
0
**
Cnt
CP
Mirin
Mirin + CP
4Gy 4h
4Gy 24h


H1975(R)
Rad51 foci/cell
20
15
10
5
0
*
Cnt
CP
Mirin
Mirin + CP
4Gy 4h
4Gy 24h

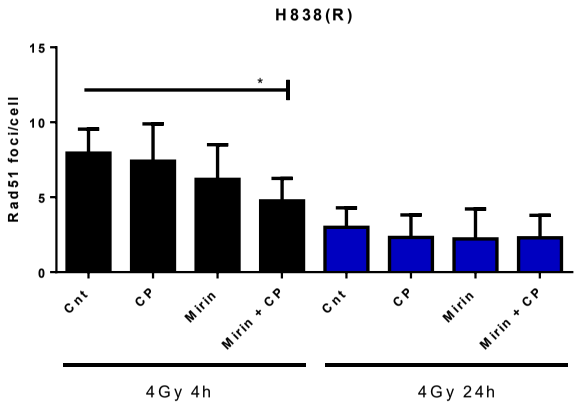

H838(R)
Rad51 foci/cell
15
10
5
0
*
Cnt
CP
Mirin
Mirin + CP
4Gy 4h
4Gy 24h

Figure 9: Effect of Cisplatin, Mirin and combined treatment on HR repair of NSCLCs. Human NSCLC cells were plated for immunofluorescence assays and were treated with 20 μM Mirin for 20 h followed by 2 μM cisplatin treatment for 4 h and were then irradiated with 0, 4 Gy prior to fixation at 4h and 24h. Rad51 foci were scored in cells co-stained with the G2-phase marker Cyclin B1. Mean ± SD of 3–4 independent experiments are shown. Statistically significant differences compared with corresponding control cells (not treated with cisplatin) are shown (*P < 0.05, **P < 0.01, ***P < 0.001).

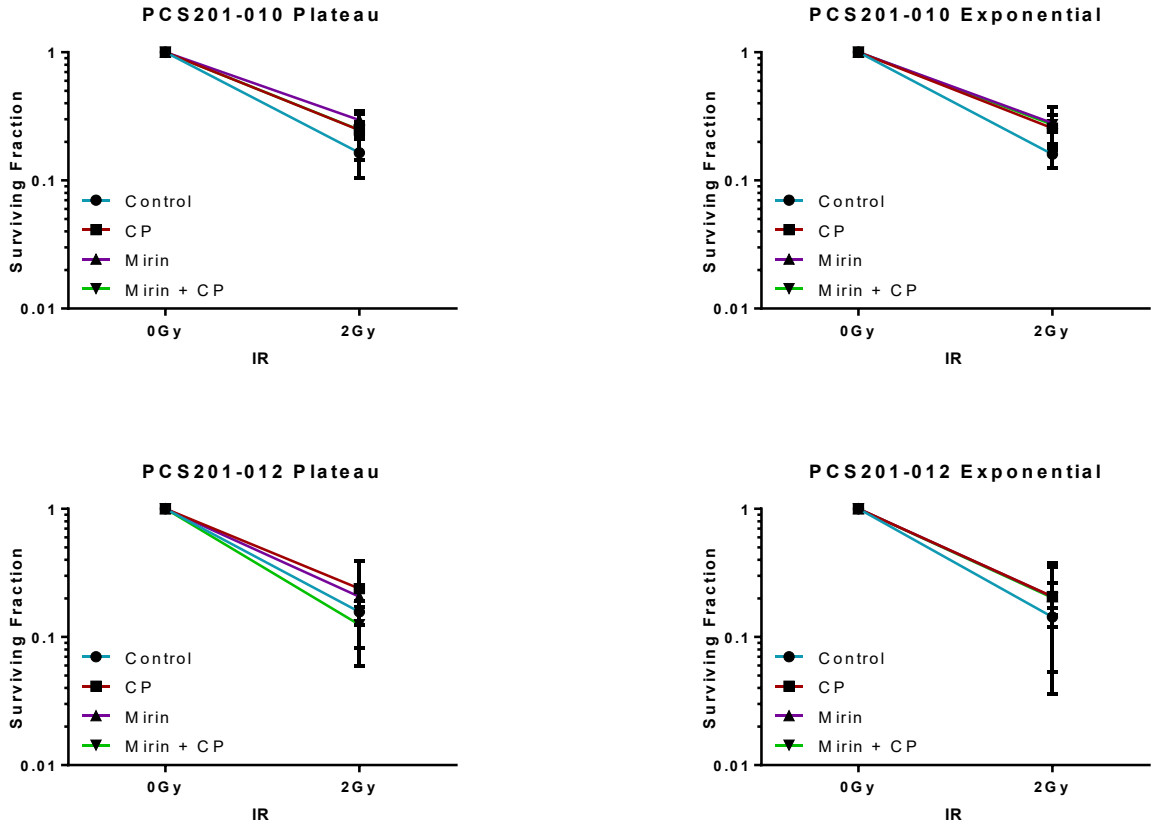


Figure 10: Effect of mirin on clonogenic survival of PCS201-010 and PCS201-012 cell lines in exponential and plateau phase state. Human fibroblasts were treated with 20 μM mirin for 20 h followed by 2 μM cisplatin treatment for 4h plated for clonogenic survival assays into mirin containing media for further 24 h Mirin treatment. After allowing the cells to attach for 4-5 h, the colonies were irradiated with 0, 2 and left for incubation with m irin containing media for 24 h. The media was replaced next day and colonies were left for incubation for 18 days. The means and standard deviation (SD) of four independent experiments are shown.

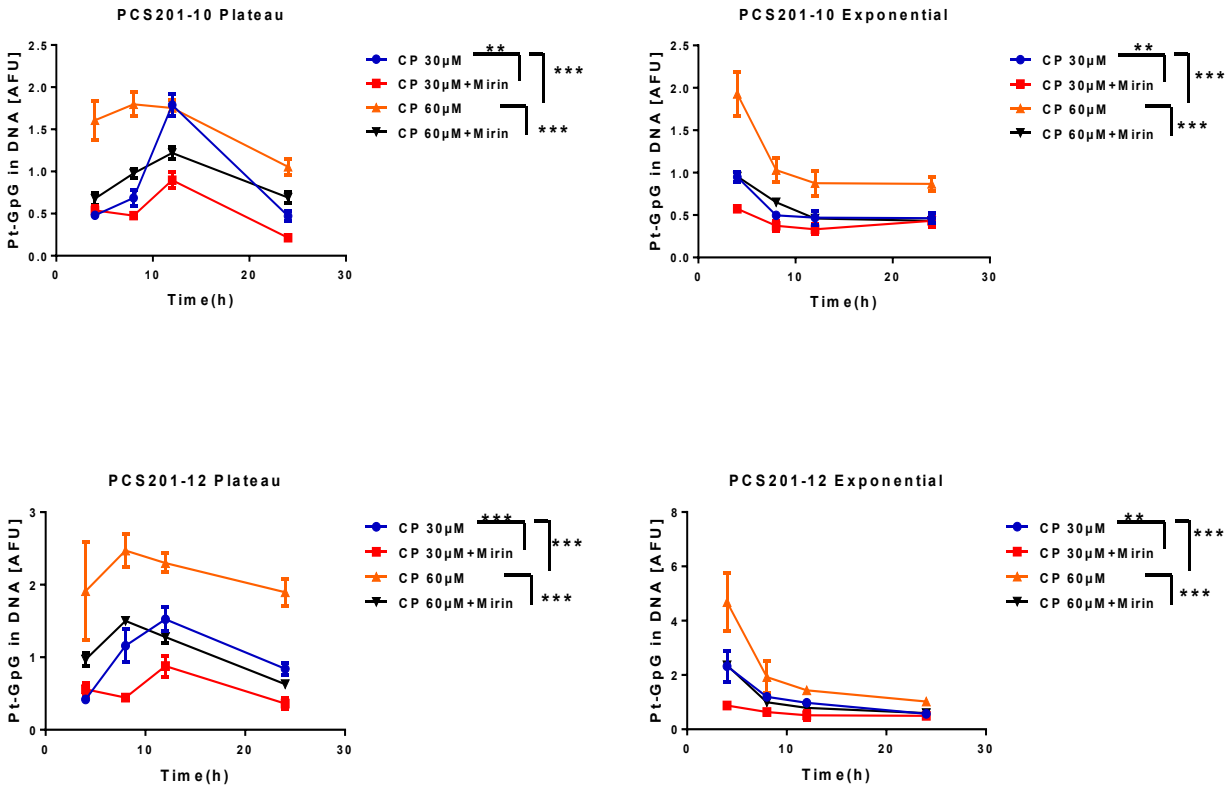


Figure 11: CP-DNA adduct kinetics after Cisplatin and Combined treatment in HDFN and HDFA. Plateau – and Exponentially growing Human DFP and DFA cells were plated for immunofluorescence assays and were treated with 20μM Mirin for 20h followed by 30μM and 60μM cisplatin treatment for 4h and fixed at 4, 8, 12 and 24h. Means + SD of 3–4 independent experiments are shown. Statistically significant differences compared with CP 30μM are shown (*P < 0.05, **P < 0.01).

Supplementary Files

This is a list of supplementary files associated with this preprint. Click to download.

- Supplemental240926.pdf